

---

## SWIMMING MECHANICS AND ENERGETICS OF ELASMOBRANCH FISHES

*GEORGE V. LAUDER*

*VALENTINA DI SANTO*

1. Introduction
2. Elasmobranch Locomotor Diversity
3. Elasmobranch Kinematics and Body Mechanics
4. Hydrodynamics of Elasmobranch Locomotion
5. The Remarkable Skin of Elasmobranchs and Its Locomotor Function
6. Energetics of Elasmobranch Locomotion
7. Climate Change: Effects on Elasmobranch Locomotor Function
8. Conclusions

The remarkable locomotor capabilities of elasmobranch fishes are evident in the long migrations undertaken by many species, in their maneuverability, and in specialized structures such as the skin and shape of the pectoral and caudal fins that confer unique locomotor abilities. Elasmobranch locomotor diversity ranges from species that are primarily benthic to fast open-ocean swimmers, and kinematics and hydrodynamics are equally diverse. Many elongate-bodied shark species exhibit classical undulatory patterns of deformation, while skates and rays use their expanded wing-like locomotor structures in oscillatory and undulatory modes. Experimental hydrodynamic analysis of pectoral and caudal fin function in leopard sharks shows that pectoral fins, when held in the typical cruising position, do not generate lift forces, but are active in generating torques during unsteady swimming. The heterocercal (asymmetrical) tail shape generates torques that would rotate the body around the center of mass except for counteracting torques generated by the ventral body surface and head. The skin of sharks, with its hard surface denticles embedded in a flexible skin, alters flow dynamics over the surface and recent experimental data suggest that shark skin both reduces drag and enhances thrust on oscillating propulsive surfaces such as the tail. Analyses of elasmobranch

locomotor energetics are limited in comparison to data from teleost fishes, and data from batoids are particularly scarce. We present an overview of comparative data on elasmobranch energetics, with comparisons to selected teleost fishes: generally, teleost fishes exhibit low costs of transport compared to elasmobranchs. Many elasmobranch species are particularly susceptible to changing oceanic conditions in response to climate change as a result of benthic habitat, reproductive mode, or reproductive site fidelity. Experimental studies on skates demonstrate that even small changes in water temperature can negatively impact locomotor performance, and locally adapted populations can differ in how they respond to abiotic stressors.

## 1. INTRODUCTION

Elasmobranch fishes exhibit remarkable locomotor diversity, sometimes forming large aggregations of individuals (Clark, 1963) for feeding and reproduction, exhibiting long distance oceanic migrations, and inhabiting ecological zones that vary from benthic to coral reefs to the open ocean. Associated with this behavioral and ecological diversity is an array of morphological and physiological adaptations that range from specialized skin structure, to the arrangement of muscle fibers in the segmental body musculature, to the structure and shape of the body wall and fins. Recent studies of elasmobranch locomotion have involved analysis of patterns of body and fin bending, how body muscles function to generate thrust, hydrodynamic effects of tail and fin movement, and analysis of the effects of the shark skin surface on swimming function. Furthermore, energetic analyses of elasmobranch swimming, while still few in number, are beginning to allow broader comparisons to teleost fishes for which a large database on the energetics of locomotion exists.

Although the topic of elasmobranch locomotion has been addressed in a number of overviews recently (Lauder, 2006, 2015; Maia et al., 2012; Shadwick and Goldbogen, 2012; Shadwick and Lauder, 2006; Wilga and Lauder, 2004a) our goal in this chapter is to focus on selected recent results, place these new data in the context of previous work, and provide some original data on locomotor hydrodynamics and batoid energetics. We conclude with a discussion of the possible effects of climate change on ocean chemistry and how this will affect locomotor function and energetics in key elasmobranch species, an area of considerable topical importance but one that has not received much previous attention.

## 2. ELASMOBRANCH LOCOMOTOR DIVERSITY

Elasmobranchs display a remarkable diversity of locomotor designs and use a variety of anatomical systems to execute some amazing feats of movement. Chimeras use pectoral fin flapping motions in addition to undulatory body undulations in a manner very similar to pectoral fin swimming in teleost fishes (Daniel, 1988). Rays swim using complex motions of their pectoral fins, which can be undulated in a wave-like motion as in stingrays (Blevins and Lauder, 2012; Rosenberger and Westneat, 1999), oscillated primarily in the vertical plane as illustrated by swimming manta rays (Moored et al., 2011a,b), or a combination of both (Rosenberger, 2001). A series of recent papers has shown how some species of skates can use their modified pelvic fins as “limbs” to push against the substrate during benthic locomotion, a behavior termed “punting” (Koester and Spirito, 2003; Macesic and Kajiura, 2010; Macesic et al., 2013; Macesic and Summers, 2012).

Most shark species possess an elongated body with one or more dorsal, pectoral, and anal fins that can be actively moved even as the body undergoes undulatory motion during swimming. The body shapes of sharks are themselves quite diverse and the classic paper by Thomson and Simanek (1977) provided the first general overview of the diversity of body shapes, and the Thomson–Simanek framework has been used by a number of subsequent authors (e.g., Shadwick and Goldbogen, 2012; Wilga and Lauder, 2004a). Dorsoventrally flattened angel sharks use expanded pectoral fins in addition to body undulation to power locomotion, while the diversity of shark body shapes includes species with classic heterocercal (asymmetrical) tail fins and fast pelagic swimmers such as lamnid sharks with a wing-like tail fin that is externally almost symmetrical in shape, with the upper and lower lobes of nearly equal area. Body shape is relevant to locomotion not only for discussions of streamlining and drag reduction in pelagic species, but also because sharks use their body and head shapes to generate lift and to regulate body torques as we discuss below. Parameters such as head shape (which can range from conical to flattened or blunt), and flattening of the ventral body surface to create lift when the body is inclined, are key to understanding the process of undulatory locomotion in sharks, which differs from that of the more completely studied teleost fishes due to differences in body density and tail shape (Maia et al., 2012).

Morphological diversity in elasmobranch body and fin shapes is associated with a great diversity of ecological locomotor behaviors which include migration across vast oceanic distances as well as diel migrations probably associated with feeding (see Chapter 8) (Graham et al., 2012; Weng and Block, 2004; Weng et al., 2007). And yet the study of

elasmobranch body form in relation to ecology and migratory patterns has just begun and is a rich area for future research (e.g., [Irschick and Hammerschlag, 2014a,b](#)).

In addition, we wish to draw attention to the relative lack of information on the routine swimming speeds of elasmobranchs (see Chapter 8) ([Lowe, 1996](#); [Parsons and Carlson, 1998](#)). There is a natural focus both in the literature and in the popular press on the high speeds and on the maximal swimming performance of fishes in general and sharks in particular. But the most ecologically relevant locomotor factor that may dictate locomotor efficiency during long migrations to reproductive sites, diel migrations, or the day-to-day search for food is the average, routine swimming speed that can be aerobically maintained at relatively low energetic cost. Such activity might take place at swimming speeds near the minimum cost of transport, but this has yet to be documented. Routine swimming speeds in many elasmobranch species are reported to be around 1 body length per second (e.g., [Parsons, 1990](#); [Parsons and Carlson, 1998](#)), and routine slow swimming in Greenland sharks (*Sommiosus microcephalus*) involves tail beat frequencies below 1 Hz ([Shadwick](#), personal communication). This may be in part due to a scaling effect of the larger body size in most elasmobranchs compared to teleost fishes, where routine swimming speeds tend to be greater than a body length per second but absolute body lengths are smaller. There is a notable lack of data on routine swimming speeds in chimaeras, skates, rays, and indeed in most shark species also. Elasmobranch species can be challenging to study ecologically under field conditions, and are not amenable to direct visual tracking to obtain routine swimming speed estimates. Tagging studies with high temporal resolution capable of recording tail beat frequencies and water flow speed past the body probably represent the main means of obtaining this information, and we hope that future work will provide a much clearer picture of the frequency distribution of swimming speeds with high temporal fidelity in a variety of elasmobranch species.

### 3. ELASMOBRANCH KINEMATICS AND BODY MECHANICS

The general descriptive terminology that is associated with elasmobranch locomotion mirrors that used to describe swimming in bony fishes ([Maia et al., 2012](#); [Shadwick, 2005](#)). Most sharks swim using body undulations in a generally “anguilliform” or eel-like mode with waves of body bending passing down the body ([Fig. 6.1](#)), although measurement of specific parameters such as body wavelength and amplitude place many shark species in the “subcarangiform” classification with the body length containing less than a half wavelength

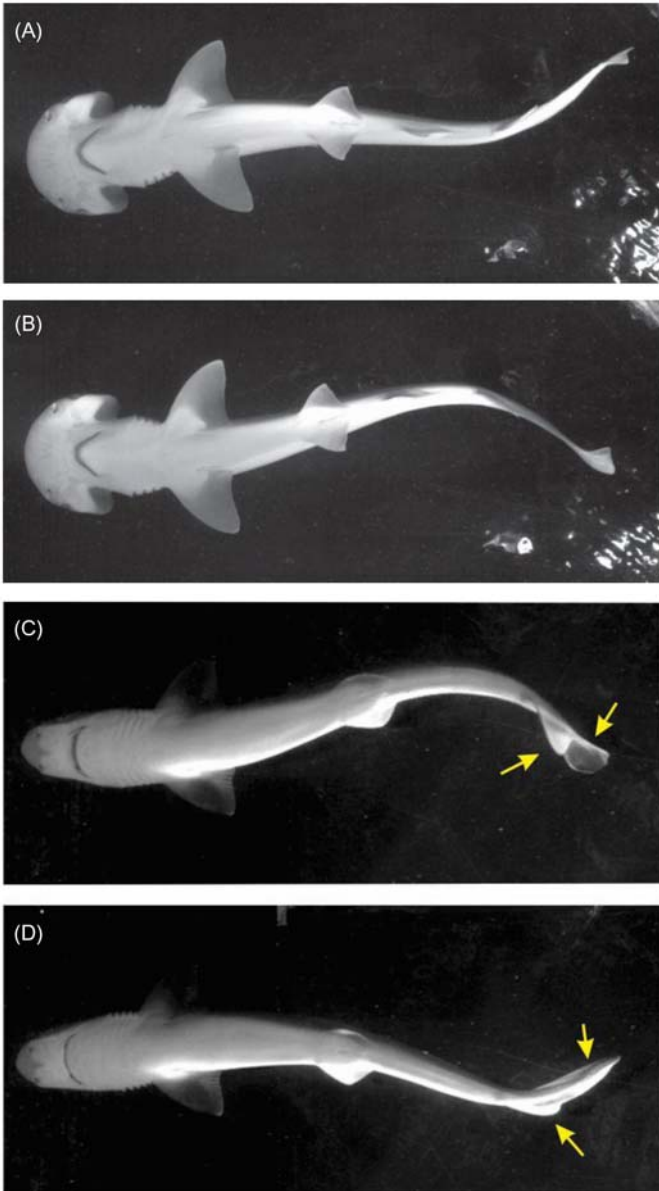


**Figure 6.1.** Undulatory locomotion using waves of body bending in swimming sharks. (A and B) Bonnethead shark (*Sphyrna tiburo*) showing body conformation at two times when the tail is approximately  $180^\circ$  out of phase during a single tail beat cycle. (C and D) Spiny dogfish shark (*Squalus acanthias*) at similar times in the tail beat cycle. Note the undulatory wave on the body and the change in shape of the heterocercal tail (yellow arrows) during swimming. From [Lauder \(2015\)](#).

(Webb and Keyes, 1982). While this classificatory terminology dates back to the classic papers of Breder (1926) and Lindsey (1978) and has been expanded in recent years to differentiate between BCF (body and caudal fin) and MPF (median and paired fin) locomotion, we believe that much of the diversity of locomotor function in fishes is obscured by this descriptive terminology.

Specifically, even during undulatory locomotion using waves of body bending, the median and paired fins of sharks play an important role in balancing pitch, roll, and yaw torques, and the dorsal fins in particular are also capable of generating thrust by accelerating water posteriorly (Maia and Wilga, 2013a,b; Wilga and Lauder, 2000). Median and paired fins in elasmobranchs are under active control by intrinsic musculature and their function during undulatory locomotion is integral to understanding how destabilizing forces are managed by swimming elasmobranchs. However, compared to the fins of teleost fishes, which possess highly flexible fin rays with a bilaminar structure that allows active bending (Lauder, 2006), elasmobranch fins with their rod-like fin rays appear to be less flexible and capable of lower curvatures and range of motion. An additional function of median fins during swimming in sharks is the interaction between flows generated by the dorsal fins and the caudal fin (Maia and Wilga, 2013a; Webb and Keyes, 1982), a phenomenon that has also been studied extensively in teleost fishes (Drucker and Lauder, 2001; Standen and Lauder, 2007). Depending on the relative timing of active dorsal and caudal fin movements, fluid vortices shed from the dorsal fins can interact with caudal fin flows to substantially alter free-stream fluid motion incident to the tail.

The roles of fins can change considerably during unsteady locomotor movements compared to their function during steady swimming. Studies of the function of shark pectoral fins, for example, have shown that fin conformations maintained during steady horizontal swimming are adjusted during vertical maneuvering in order to generate torques that pitch the body up or down (Fish and Shannahan, 2000; Wilga and Lauder, 2000, 2001), which facilitates vertical movement in the water column. Control of pitching body motions may be especially important in elasmobranchs, which tend to be negatively buoyant and lack the gas-filled swimbladder common to most teleost fishes.

Batoid fishes are known for their use of pectoral fins during locomotion (Blevins and Lauder, 2012; Fontanella et al., 2013; Klausewitz, 1964; Parson et al., 2011; Rosenberger, 2001), and skates and rays also show changes in fin and body position during transitions from steady horizontal swimming to vertical maneuvering. Study of locomotion in skates illustrates the changing role that fins can take when maneuvers are initiated and during vertical movement. In the little skate, *Leucoraja erinacea*, steady horizontal locomotion occurs via wave-like motions of the expanded pectoral fins (Fig. 6.2). Although pectoral fin motion is generally wave-like, the shape of the pectoral fin changes considerably between downstroke and upstroke

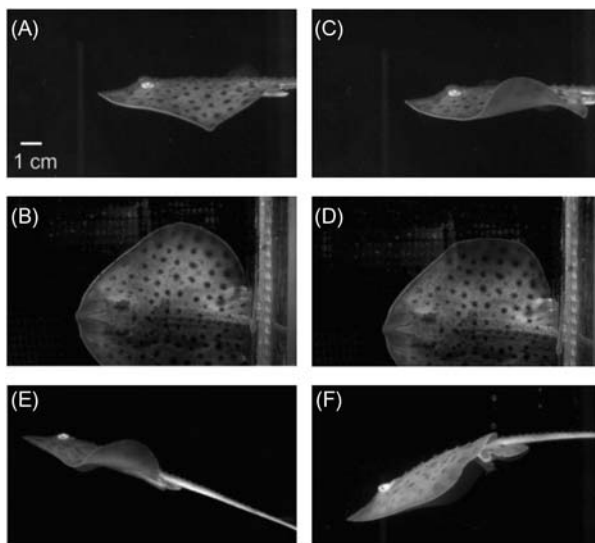


**Figure 6.2.** Swimming kinematics in the little skate, *Leucoraja erinacea*. (A and B) Frames from high-speed video recordings of body and pectoral conformations during steady horizontal locomotion at a swimming speed of 1.2 BL/s. (C and D) Body and pectoral fin conformation at a time 0.24 s after the images shown in (A) and (B). Note the change in pectoral wave shape. (E and F) Body and pectoral conformation during vertical (ascending) locomotion (E), and during downward (ventral) descent (F). Ascending is active and often accompanied by high amplitude and rapid pectoral fin motions, while descending can be passive following body reorientation at a negative angle of attack to oncoming flow.

(compare Fig. 6.2, panels A and C). Lateral views show that during the downstroke, a relatively sharp transition point can occur in the middle of the fin margin as the wave is propagated posteriorly (Fig. 6.2A). During the upstroke, the fin margin takes on a more rounded shape (Fig. 6.2C); the effect of these downstroke–upstroke shape changes on patterns of fluid flow and force production are as yet unknown.

Fin kinematics in the little skate show some interesting changes while executing vertical maneuvers. Ascending in the water column is actively powered by higher amplitude fin wave-like motions than those used during steady forward swimming (Fig. 6.2E). However, descending occurs by reorienting the body at a negative angle of attack and is largely passive with only low amplitude movements of the pectoral fins (Fig. 6.2F). Very few kinematic studies of locomotion in freely swimming skates or rays are available, so it is not currently possible to say how general these observations are.

An additional noteworthy aspect of pectoral fin locomotion in batoids was described by Blevins and Lauder (2012) in their study of three-dimensional

pectoral fin kinematics in the freshwater stingray *Potamotrygon orbignyi*. They observed that the outer margin of pectoral fin, during the downstroke, can be rather substantially cupped downward, and hence curved into the flow. If pectoral fin kinematics were dominated by the fluid loading occurring as the fin is moved down against the fluid, then the fin margin would be expected to be curved upward as is seen on the pectoral fin in the oscillatory motion of manta rays. But the opposite conformation often occurred in the freshwater stingray, and suggests that active control of the fin margin allows detailed shape changes during swimming, which perhaps function to control how water flows over the fin edge and to increase thrust by directing more water posteriorly.

Batoids are also noted for benthic locomotion where fin movements occur near the substrate and are subject to “ground effect” hydrodynamic influences. Ground effects are well known for flying animals and man-made aircraft where both rigid and flapping wings alter flows near surfaces (see review in [Rayner, 1991](#)), but the dynamics of aquatic animals interacting with the substrate are very different given the flexible undulating propulsive modes observed in fishes. The ground effect has proven challenging to study in live elasmobranchs, but several recent papers have addressed some of the kinematic and hydrodynamic factors involved with rays swimming in ground effect using simple physical models. Studies using flexible membranes as models of ray wings, either with dual actuators driving a rubber membrane ([Blevins and Lauder, 2013](#)) or a single leading edge actuator controlling a flexible panel ([Quinn et al., 2014a,b](#)), have shown that swimming near the bottom can greatly alter flow patterns over the undulating membrane. Remarkably, even though kinematics of the membranes can remain relatively unchanged, substantial improvements in swimming efficiency can be achieved.

In sharks the function of the asymmetrical (heterocercal) shape of the tail received renewed attention beginning with the paper by [Thomson \(1976\)](#) who first suggested that the asymmetrical shape acts to direct locomotor force through the center of body mass and thus avoids inducing rotational torques tending to pitch the head down. This contrasts with the classical view that the heterocercal tail generates lift forces ([Affleck, 1950](#)). The heterocercal tail moves in a complex manner ([Fig. 6.1C and D](#): yellow arrows) and requires a full three-dimensional study to determine the orientation of different regions of the tail during swimming. Experimental analysis of three-dimensional motion of the heterocercal tail in leopard sharks ([Ferry and Lauder, 1996](#)) suggested that the classical model was correct, and that orientation of the tail surface during side-to-side movement indicates that lift forces are produced, which pitch the head ventrally around the center of mass (COM). However, confirmation of this suggestion based

on kinematics required subsequent experimental studies of fluid flows generated by the tail and calculation of the direction of reaction forces on the body. We consider those results in the next section along with implications for body dynamics in swimming sharks.

One aspect of elasmobranch locomotion that has received little attention is the analysis of unsteady locomotor behaviors such as accelerations and escape responses. [Domenici et al. \(2004\)](#) analyzed escape responses in spiny dogfish and [Seamone et al. \(2014\)](#) have recently used a predator model to induce escape responses in the same species. Spiny dogfish show generally similar c-start escape patterns to those of teleost fishes, although variability among responses is relatively high and the speed of the response was slower than values typical for teleost fishes. Escape and turning performance has been analyzed quantitatively in rays by [Parson et al. \(2011\)](#) and in sharks by [Maia and Wilga \(2013b\)](#), [Porter et al. \(2009, 2011\)](#), [Shadwick and Goldbogen \(2012\)](#), and [Kajiura et al. \(2003\)](#). Further analysis of unsteady swimming behaviors, which may in fact be among the most common locomotor events in the daily repertoire, is very much needed to round out the picture of elasmobranch swimming diversity.

The study of elasmobranch body mechanics from the perspective of material design and function has progressed greatly in recent years. Elasmobranch skeletal mechanics in particular has received attention, and the functional design of the batoid wing ([Dean et al., 2009; Dean and Summers, 2006](#)) and shark vertebral elements ([Porter and Long, 2010; Porter et al., 2006, 2007, 2014](#)) have been used as inspiration for the design of vertebral columns that serve as models for flexible mechanical devices and for evolutionary analyses of alternative undulatory designs ([Liu et al., 2010; Long et al., 2006, 2011](#)).

Understanding the mechanics of how undulatory body motions are achieved in elasmobranchs has come a long way since the classic paper by [Bone \(1966\)](#) used electromyography in dogfish, *Scyliorhinus canicula*, to show the division of labor between red and white myotomal fibers as swimming speed increases. His paper demonstrated convincingly that red, aerobic, muscle fibers were used for slow-speed swimming, while the larger glycogen-containing and deeper white fibers that make up the majority of myotomal volume were used for high-speed swimming and unsteady movements (also see subsequent papers that elaborate on this original result; [Bone, 1978, 1988, 1999; Bone et al., 1978](#)). [Donley and Shadwick \(2003\)](#) followed up the work of Bone with a comprehensive analysis of red muscle function that included measurement of fiber strain with sonomicrometry and quantification of body bending kinematics to show that the pattern of red muscle activation was consistent along the body for slow to moderate speed swimming and contributed to positive power along the

length, unlike previous results obtained for many teleost fishes. Recent overviews of shark muscle function can be found in [Shadwick and Gemballa \(2006\)](#), [Shadwick and Goldbogen \(2012\)](#) and [Syme \(2006\)](#) (see also Chapter 5).

Analysis of the mechanics of shark musculature changes considerably when fast-swimming pelagic species such as lamnid sharks are considered because the red muscle is internalized and located medially ([Bernal et al., 2003a,b](#); [Graham et al., 1994](#); [Sepulveda et al., 2005](#)), and these red fibers possess an elevated temperature with respect to ambient water ([Bernal et al., 2005, 2009](#); see also Chapter 8). The remarkable evolutionary similarity between pelagic lamnid sharks and tuna ([Bernal et al., 2001](#); [Donley et al., 2004](#); [Shadwick, 2005](#)) in the location of the red musculature and in the attachment of body muscle fibers to collagenous myosepts is one of the most outstanding known examples of convergent biomechanical evolution.

#### 4. HYDRODYNAMICS OF ELASMOBRANCH LOCOMOTION

Experimental analyses of water flow over the bodies and fins of swimming elasmobranchs have enabled a number of hypotheses about body and fin function to be addressed. Quantitative flow visualization borrows approaches from engineering to visualize and analyze patterns of water movement over the surface and in the wake of the body and fins ([Drucker and Lauder, 1999](#)). In swimming leopard sharks, [Wilga and Lauder \(2002, 2004b\)](#) showed that the heterocercal tail generated a momentum jet that is directed posteriorly and ventrally, and thus produces a reaction force aimed above the center of mass (COM) ([Fig. 6.3](#)). This confirmed the canonical model of heterocercal tail function and indicates that the classic heterocercal tail shape generates lift forces and body torques. [Flammang et al. \(2011\)](#) applied a recently developed volumetric flow imaging approach to heterocercal tail function and showed a more complex vortex wake signature than previously suspected ([Fig. 6.3D](#)), while confirming earlier work on the direction of forces and the momentum jet produced by heterocercal tails ([Fig. 6.3E](#)). [Borazjani and Daghooghi \(2013\)](#) have shown an important additional feature of fish tails that applies to both heterocercal and homocercal tail hydrodynamics: the tail appears to generate an attached leading edge vortex that enhances thrust in a manner similar to proposed previously for insect and bird wings. The significance of differences in shape between the upper and lower lobes in the heterocercal tail for leading edge vortex structure is as yet unknown, but the computational fluid dynamic approach promises new insights into the function of elasmobranch caudal fins.

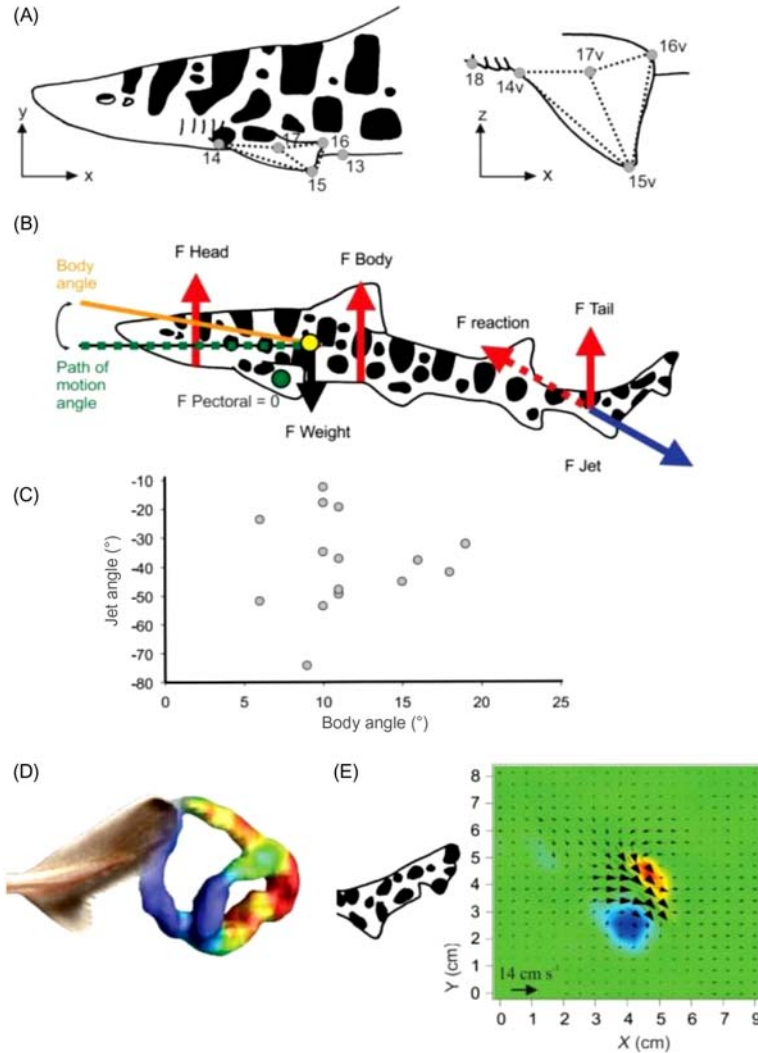


**Figure 6.3.** Dynamics of locomotion in sharks studied with three-dimensional (3D) kinematics and particle image velocimetry. (A) 3D analysis of pectoral fin conformation in swimming leopard sharks (*Triakis semifasciata*, 21–26 cm total length) shows that the pectoral fins are held in a position that generates minimal vorticity during steady swimming. (B) Summary of forces acting on the body of a steadily swimming shark (see text for discussion). (C) Plot of the angle of the fluid dynamic jet formed by the tail vortex ring versus body angle. Jets are negative (below the horizontal) no matter what the body angle in leopard sharks, which indicates that the tail generates torques around the center of mass. These torques are counteracted by lift forces on the body. (D) Vortex ring conformation generated by one tail beat in a swimming spiny dogfish (*Squalus acanthias*). (E) Vertical slice through the vortex wake of a swimming leopard shark showing two centers of vorticity and the central fluid jet inclined below the horizontal. Modified from Flammang et al. (2011) and Wilga and Lauder (2000, 2002).

Data on flow visualization over the body and pectoral fins (Wilga and Lauder, 2000) combined with analysis of flows generated by the tail provide an overall picture of the balance of forces on the body of freely swimming sharks (Fig. 6.3). During steady horizontal locomotion, pectoral fins are held in a conformation that results in near zero net lift forces (Fig. 6.3A). However, this changes dramatically during maneuvering when pectoral fins change their angle of attack to initiate pitch moments about the COM.

During horizontal steady swimming, the body is inclined to the horizontal and generates lift forces and also counter-rotating torques around the COM (Fig. 6.3B). Both net lift and torques must balance and this is achieved dynamically during each tail beat as the head, body, and tail lift forces match gravitational forces, and oppositely-signed torques balance to prevent net rotation (Fig. 6.3B). In leopard sharks, the angle of the fluid dynamic tail jet is independent of the angle of the body during swimming, while in bamboo sharks, *Chiloscyllium punctatum*, Wilga and Lauder (2002) observed changes in jet angle, which became more horizontal as body angle increased during slow speed swimming. Sharks adjust their body angle as swimming speed changes, and during slow horizontal swimming at 0.5 L/s the body may be inclined at an angle of approximately  $10^\circ$  or more, while at a speed of 2.0 L/s the body is nearly horizontal. However, a cautionary note is in order here. Studies that generate accurate kinematic data on the body and fins of elasmobranchs necessarily involve using smaller animals that are suitable for laboratory flumes and camera arrangements, and it is still unclear if these conclusions apply to larger freely-swimming sharks in unrestricted open-ocean conditions.

The heterocercal tail of sharks has also inspired the construction of simple physical models that have been used to understand some of the basic kinematic and hydrodynamic properties of propulsive surfaces with angled trailing edges as compared to homocercal (externally symmetrical) shapes (Lauder et al., 2011, 2012). Interestingly, analysis of the self-propelled speeds of simple flexible plastic panels with different trailing edge shapes showed that the heterocercal shape had increased swimming speeds (approximately 7% faster on average) compared to panels with the same area but a vertical trailing edge. However, this occurs with a slightly increased cost of transport (Lauder et al., 2011), and the vortex wake shed by the heterocercal panel differed in several ways from that of freely swimming leopard sharks. This difference could be due to obvious differences in structure between the simple plastic panel models and the tail of live sharks, and also to active stiffening via muscle fibers intrinsic to the tail and changes in stiffness through pressure changes in the tail as sharks swim (Flammang, 2010).

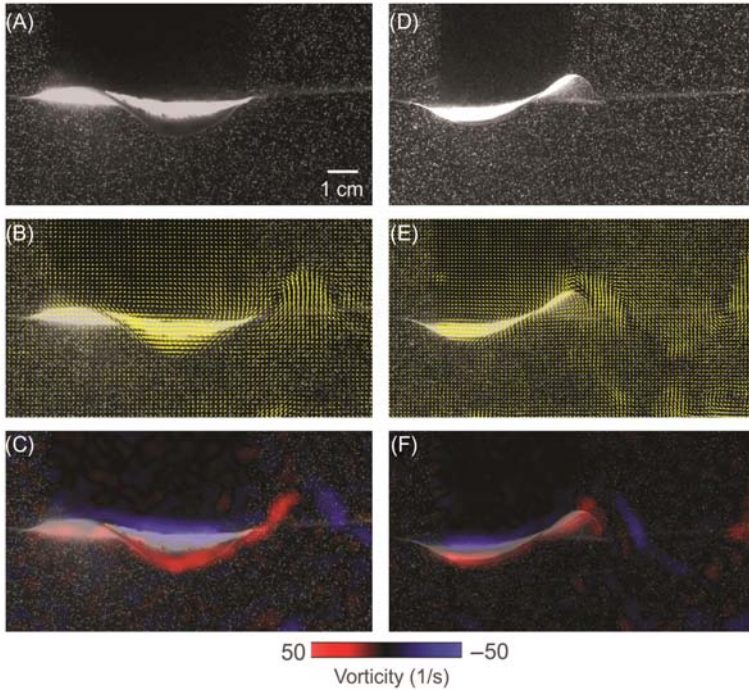


**Figure 6.4.** Hydrodynamics of locomotion in the little skate, *Leucoraja erinacea*, swimming at 2.0 BL/s. This individual has a disk length of 8.5 cm. (A–C) Position of the body and pectoral fin in the laser light sheet with particles illuminating the flow to allow particle image velocimetry analyses (A), velocity vector field at this time with free-stream flow subtracted (B), and vorticity generated by pectoral fin motion (C). (D–F) Comparable images at a time 0.56 s later in time.

Experimental hydrodynamic data on batoid locomotion are not currently available for live animals swimming steadily, and most hydrodynamic data relevant to skate and ray swimming come from panel models or robotic systems (Moored et al., 2011a,b). Here we present experimental hydrodynamic measurements of flow around the body and in the wake of the little skate, *L. erinacea*, during steady locomotion at a moderate swimming speed of 2.0 L/s (Fig. 6.4). Particle image velocimetry of flows around the body and wake of the undulating pectoral fins shows clear momentum jets that alternate from posterodorsal to posteroventral (compare Fig. 6.4, panels B and E). These momentum jets are not symmetrical and jet velocities resulting from the upstroke appear to be of higher speed and carry greater momentum than downstroke flows. In addition to the associated vortex wake, flow slowed by interaction with the body and wing is evident as ribbon-like strips of vorticity over the upper

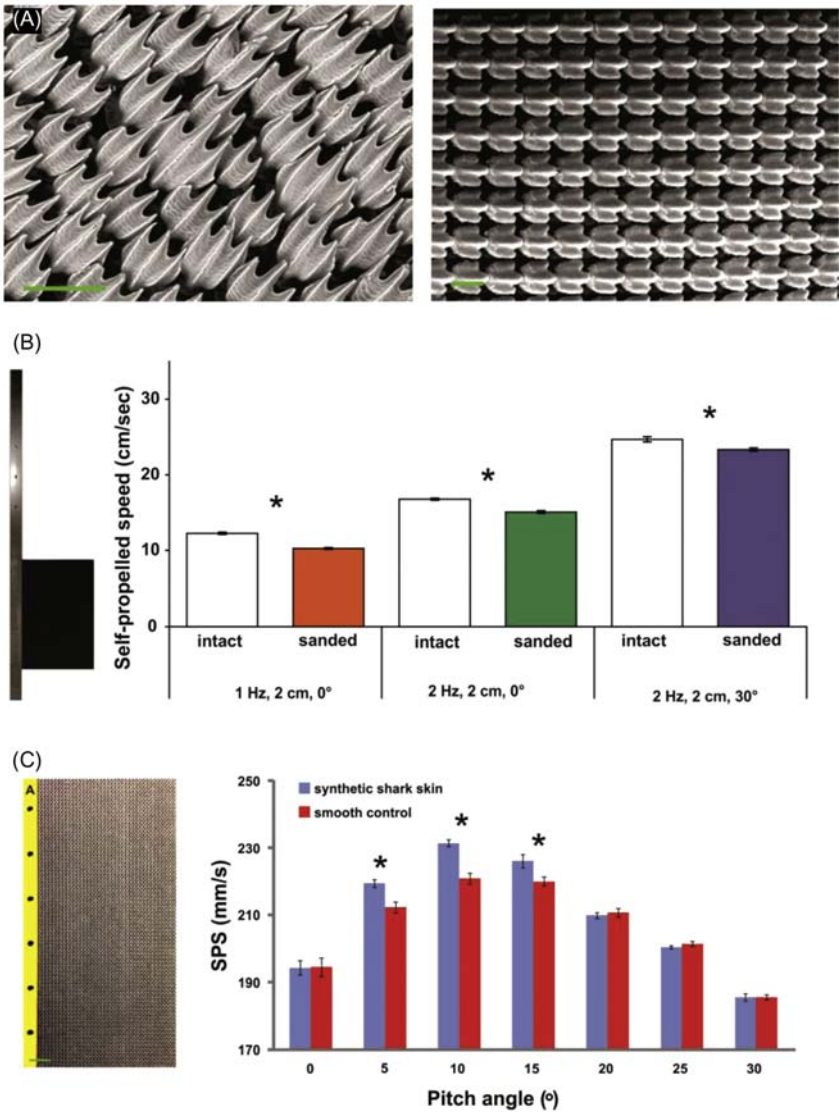


**Figure 6.5.** Structure and function of the denticles (scales) on the skin of a bonnethead shark (*Sphyrna tiburo*) and manufactured biomimetic model shark skin. (A) Left panel, environmental scanning electron microscope image of skin denticles near the anal fin (green scale bar=200  $\mu$ ) of a bonnethead shark (*Sphyrna tiburo*); right panel, scanning electronic microscope image of fabricated biomimetic synthetic shark skin used for hydrodynamic testing. Artificial shark skin is produced using additive manufacturing (3D printing); green scale bar=1 mm. (B) Dynamic testing of the hydrodynamic function of shark skin denticles using pieces of shark skin that are

body and lateral pectoral edge (Fig. 6.4C). These preliminary data suggest that further studies including a diversity of batoid species would be useful for understanding how different patterns of pectoral fin motion and body positions alter flows produced by the pectoral fins, and the relative balance of upstroke and downstroke momentum production.

## 5. THE REMARKABLE SKIN OF ELASMOBRANCHS AND ITS LOCOMOTOR FUNCTION

As the fin and body surfaces of elasmobranchs undulate and are moved through the water, the skin encounters a time-dependent flow pattern. Friction between skin and the water is likely to be an important (although still of unknown magnitude) source of drag, and there is now a large literature on how the skin of elasmobranchs might have special drag-reducing properties. Much of this literature is based on engineered models (Bechert et al., 1986; Bechert and Hage, 2007; Dean and Bhushan, 2010) and shows that surface texture, of an appropriate size and spacing, can result in drag reduction as fluid is moved steadily past a textured surface.

Shark skin has inspired much of this research on the function of surface texture due to its remarkably complex structure (Kemp, 1999; Liem et al., 2001; Motta et al., 2012; Reif, 1982, 1985). Small (100  $\mu\text{m}$  to 1 mm) bony dermal denticles (Fig. 6.5A) cover the skin. Denticles are embedded into the dermis (Kemp, 1999; Motta, 1977) with a small expanded bases, and have stalk-like structures that extend through the skin to support ridged flanges exposed to water flow at the surface (Fig. 6.5A).

Although studies of shark skin models under static conditions where the textured surface does not move have provided a solid baseline of data on

attached to a flat support (shown on the left) which in turn is attached to a mechanical flapping foil device that allows controlled side-to-side and rotational motions of the shark skin membrane. Graph shows the self-propelled swimming speed of the shark skin membrane with intact denticles and after the denticles have been sanded off (to produce a relatively smooth surface) under three different motion programs. Note that in each case the swimming speed of the shark skin with denticles intact is significantly greater (\*) than after the denticles have been removed by sanding. (C) Assembly of the tested flexible biomimetic shark skin foil (on left) and hydrodynamic analysis. A flat support attaches to the yellow area with holes on the left side of the foil, and this support is moved by a mechanical flapping device. Graph of the results from measuring the self-propelled swimming speed of the biomimetic shark skin foil (blue bars) compared to the smooth control (red bars) at different pitch angles. Heave motion was  $\pm 1.5$  cm at 1 Hz for all trials. At pitch angles of 5°, 10°, and 15° the biomimetic shark skin foils swim significantly faster (\*) than the smooth controls. At the other four pitch angles, the swimming speeds are similar. Modified from Oeffner and Lauder (2012), Wen et al. (2014), and Lauder (2015).

drag reduction, the lack of dynamic testing is of special concern. Shark skin, during free-swimming, is exposed to time-dependent flows with changing angles of attack and also flow separation over leading edges of the fins and tail, and also possibly along the body (Anderson et al., 2001). This suggests that dynamic testing is needed where skin and biomimetic versions of shark skin can be moved under a controlled motion program that mimics that of freely-swimming sharks, and forces, fluid flow patterns, and swimming performance measured. Wen et al. (2014) manufactured a biomimetic shark skin, and tested its function in comparison to a smooth control (Fig. 6.5A, right panel). Manufactured shark skin mimics have the advantage of allowing good experimental control, as smooth surfaces with the same mass as the artificial skin can also be studied and swimming performance compared.

Oeffner and Lauder (2012) used pieces of real shark skin to make flexible membranes attached to a supporting rod (Fig. 6.5B). By attaching this rod to a computer controlled mechanical flapping apparatus (Lauder et al., 2007, 2011) that allows dynamic testing, they were able to move the pieces of shark skin in an undulatory motion program with realistic angles of attack and to achieve curvatures of the shark skin that match that of freely-swimming sharks. They found that the textured denticle surface increased swimming speed by an average of 12.3% compared to a smoothly sanded control in which the denticles have been removed, moving with the same motion program of heave and pitch (Fig. 6.5B). An additional key result was that the increased swimming speeds did not occur in shark skin membranes that were attached to rigid surfaces, indicating that flexibility and bending of the shark skin membrane is critical to the increased performance with the roughened denticle surface.

Analysis of the flow field around swimming shark skin membranes and the sanded controls revealed a possible new role for the denticle-covered shark skin surface. Oeffner and Lauder (2012) found changes in the intensity and location of the leading edge vortex attached to the swimming shark skin membrane suggesting that the roughened surface might enhance thrust by promoting leading edge suction compared to a smooth control. They hypothesize that this effect may have been at least partially responsible for the observed increased swimming speeds, and may apply to regions of the shark body where flow separation occurs, such as the tail.

One limitation of studying real shark skin is that it is difficult to modify the denticle pattern and make experimental alterations to determine which specific features of shark denticles most affect swimming mechanics. To address this issue, Wen et al. (2014) manufactured a biomimetic shark skin and smooth controls and compared their performance under dynamic swimming conditions. Fig. 6.5C shows how the self-propelled swimming

speed of the biomimetic shark skin and smooth controls compares when moved at a constant heave of  $\pm 1.5$  cm at 1 Hz under a variety of different pitch angles. Manufactured shark skin swam significantly faster at pitch angles of  $5^\circ$ ,  $10^\circ$ , and  $15^\circ$ , but at the same speed as the smooth control at low ( $0^\circ$ ) and high ( $20$ – $30^\circ$ ) pitch angles. The effect of the shark skin surface on locomotor performance thus depends critically on the motion program and how the surface interacts dynamically with oncoming flow as it moves through water.

These results suggest that the function of the roughened denticle-covered skin of sharks is complex and motion-dependent, and it is clear that much more remains to be discovered about the diversity of denticle patterns over the body and among species, the effect of possible movement of individual denticles during swimming (Lang et al., 2008, 2014), and the functional significance of the ornamentation on the denticle surface.

## 6. ENERGETICS OF ELASMOBRANCH LOCOMOTION

Studies that estimate the energetic costs incurred by elasmobranchs during swimming are scarce. In a few cases, costs of locomotion have been measured using a Brett-type swim tunnel (Brett, 1971), although recent technological advances have allowed researchers to approximate energetic costs in free-swimming sharks using speed and tail-beat sensors that have been calibrated to oxygen consumption rates (e.g., Graham et al., 1990; Scharold and Gruber, 1991; Sepulveda et al., 2004; Bernal et al., 2012; see also Chapter 8). Most studies on the metabolism of elasmobranchs have focused on a few benthic and inactive species, resting on the bottom of a respirometer (resting metabolic rate; Brett and Blackburn, 1978; Ferry-Graham and Gibb, 2001; Di Santo and Bennett, 2011b). However, some studies also measured resting metabolic rates of more active sharks, such as the mako shark, which exhibit oxygen consumption rates at rest similar to comparably sized yellowfin tuna *Thunnus albacares* (240 vs. 253 mg O<sub>2</sub> × kg<sup>-1</sup> h<sup>-1</sup>, respectively; Graham et al., 1990; Dewar and Graham, 1994). A few other researchers have used swim tunnels to measure swimming metabolic rates in sharks. The metabolic rates of elasmobranchs during steady swimming have been reported for mako (Graham et al., 1990; Sepulveda et al., 2007), leopard (Scharold et al., 1988a), lemon (Scharold and Gruber, 1991), blacknose sharks (Carlson et al., 1999), and for one batoid, the little skate (Di Santo and Kenaley, in preparation), and these comparative data are summarized in Fig. 6.6 and Table 6.1. The little skate exhibits lower energetic costs during steady swimming when compared to more active ectothermic and lamnid sharks. Oxygen consumption decreases somewhat in the little skate as a function of

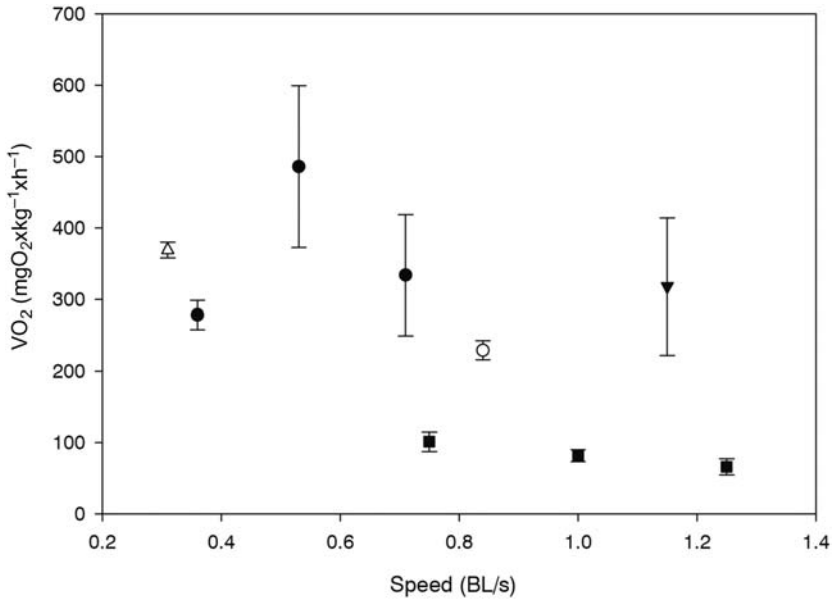


**Figure 6.6.** Oxygen consumption rates ( $VO_2 \pm SE$ ) of five species of elasmobranchs at different swimming speeds (in Body Lengths per second, BL/s): open triangle: *Isurus oxyrinchus* (Graham et al., 1990); closed triangle: *Negaprion brevirostris* (Scharold and Gruber, 1991); open circle: *Triakis semifasciata* (Scharold et al., 1988); closed circle: *Carcharhinus acronotus* (Carlson et al., 1999); closed square: *Leucoraja erinacea* (Di Santo and Kenaley, unpublished data).

speed within the range tested (0.75–1.25 BL/s). It is possible that the slightly higher metabolic rates of skates swimming at the lowest speed (Fig. 6.6) may be due to the fact that they were swimming below the velocity necessary to maintain hydrostatic equilibrium (Bernal et al., 2012), and thus incurred additional costs to maintain body stability. Even though there are only a few studies on elasmobranch energetics during activity, it is apparent that there is a positive association between fast-swimming fishes and swimming metabolic rates (Table 6.1). For instance, even after adjusting for temperature and body size, scalloped hammerhead sharks *Sphyrna lewini* consume nearly double the amount of oxygen that leopard sharks use when both are swimming about 1 body length per second (Scharold et al., 1988; Lowe, 1996, 2002).

Basic measures of oxygen consumption such as the resting metabolic rate and active metabolic rate are useful for a gross determination of the costs of activity in a species. However, calculating the aerobic scope (i.e., the difference between the maximum and the resting metabolic rates) can be used to estimate the capacity for activity in fishes (Fry, 1947; Farrell et al., 2008, 2009; Roche et al., 2013). Not surprisingly, lamnid sharks exhibit high

**Table 6.1**

Summary of resting metabolic rates (RMRs), swimming or active metabolic rates (AMRs), and cost of transport (COT) for elasmobranchs and selected teleosts

Species	Temperature (°C)	Mass (kg)	RMR ( $\text{mgO}_2 \times \text{h}^{-1} \times \text{kg}^{-1}$ )	AMR ( $\text{mgO}_2 \times \text{h}^{-1} \times \text{kg}^{-1}$ )	COT ( $\text{kJ} \times \text{kg}^{-1} \times \text{km}^{-1}$ )	Behavior and speed	Reference
<i>Anguilla anguilla</i>	19	0.155	42.21	62.71	0.62	Steady swimming 0.5 BL/s	van Ginneken et al. (2005)
<i>Oncorhynchus mykiss</i>	19	0.161	–	130.4	2.73	Steady swimming 0.7 BL/s	van Ginneken et al. (2005)
<i>Negaprion brevirostris</i>	25	1.39	152.6	240.2	3.84	Swimming 0.4 BL/s	Scharold and Gruber (1991)
<i>Triakis semifasciata</i>	–	–	105	229	–	Swimming 0.84 BL/s	Scharold et al. (1988)
<i>Isurus oxyrinchus</i>	16.5–19.5	4.4–9.5	344	541	3.79	Swimming 0.65 BL/s	Sepulveda et al. (2007)
<i>Squalus</i>	10	2	32.4	88.4	–	Swimming speed not controlled	Brett and Blackburn (1978)
<i>Scyliorhinus stellaris</i>	17.8–19.3	2.5	92	162	–	Steady swimming 0.27 BL/s	Piiper et al. (1977)
<i>Scarus schlegeli</i>	26–27	0.243	127	–	2.39	$U_{\text{crit}}$ 2.3 BL/s	Korsmeyer et al. (2002)
<i>Rhinecanthus aculeatus</i>	26–27	0.106	74.7	–	1.74	$U_{\text{crit}}$ 1.5 BL/s	Korsmeyer et al. (2002)
<i>Sphyrna lewini</i>	22–28	5.90–12.21	–	273.9	1.45	Free-swimming 0.81 BL/s	Lowe (2002)
<i>Leucoraja erinacea</i>	15	0.009	35.54	69.5	3.8	Steady swimming 1.25 BL/s	Di Santo and Kenaley (in Preparation)

active metabolic rates (Fig. 6.6) which correlate with long-distance migrations and the ability to catch fast-moving prey (Bonfil et al., 2005; Sepulveda et al., 2007; Jorgensen et al., 2010). Lamnid sharks also exhibit relatively high resting metabolic rates to accommodate morphological and physiological adaptations for high swimming performance. In fact, it has been estimated that white sharks use about 46% of their total energy intake just to sustain basal metabolic demands (Ezcurra et al., 2012).

The deployment of small activity loggers has enabled measurement of the costs of locomotion in free swimming fishes (Scharold et al., 1988; Scharold and Gruber, 1991; Farrell et al., 2008; Gleiss et al., 2010). Although precise speed sensors, accelerometers, and heart-rate monitors are now available and can be calibrated with standard swimming tests in the laboratory, there are many abiotic and biotic factors that can alter metabolic and heart rates in fishes beside swimming speed. It is unlikely that an elasmobranch would swim constantly at the same depth and in the same area, and it is therefore likely to encounter a variety of thermal environments, salinities, pH, and dissolved oxygen levels. All these abiotic factors are known to affect physiological processes in fishes (Fry, 1971; Carlson and Parsons, 2001; Meloni et al., 2002; Farrell et al., 2008; Di Santo and Bennett, 2011a; Di Santo, 2015). In addition, the presence or absence of predators, prey, and conspecifics can alter cost of activity (Wurtsbaugh and Li, 1985; Trudel et al., 2001; Allan et al., 2013; Binning et al., 2013). These factors make interpreting the data obtained from loggers challenging, but for pelagic elasmobranchs there is often little alternative.

The energetics of steady free swimming in elasmobranchs can be quite difficult to measure, especially in benthic species that are ordinarily mostly sedentary, and an alternative measure of locomotor capacity can be obtained by measuring excess post-exhaustion oxygen consumption in fishes that have been manually chased (Cutts et al., 2002; Svendsen et al., 2011; Roche et al., 2013). In this protocol, researchers gently and repeatedly tap the fish thus eliciting “burst-and-glide” swimming until the fish is unresponsive to handling, that is, fatigue is achieved, and the fish is immediately transferred to a respirometer to measure the “oxygen debt” accumulated as a result of intense short exercise (Svendsen et al., 2011; Clark et al., 2013; Di Santo, in review). For many benthic species, this method represents, to date, the only effective way to measure maximum metabolic rates, and it also may result in higher oxygen consumption rates than those measured during swimming, allowing a better estimation of maximal aerobic capacity (Clark et al., 2013; Roche et al., 2013). In the section ‘Climate Change: Effects on Elasmobranch Locomotor Function’ we describe results from this method applied to the little skate in an effort to understand the effects of changing oceanic conditions on locomotor energetics.

Finally, we emphasize that there is a near total lack of studies on the cost of locomotion in batoids, and the data shown in Fig. 6.6 for the little skate represent the only measurements that we are aware of. Without broader taxonomic representation of elasmobranch energetic data, we will not be able to make general conclusions as to energetic underpinnings associated with different modes of locomotion, and this is an especially fruitful area for future research.

## 7. CLIMATE CHANGE: EFFECTS ON ELASMOBRANCH LOCOMOTOR FUNCTION

Since the industrial revolution, global atmospheric carbon dioxide (CO<sub>2</sub>) concentrations have increased from 280 to about 400 ppm (in 2015), thus reaching levels that have not been experienced in the past 65 million years (IPCC, 2013). The two major consequences of the accelerating increase in atmospheric CO<sub>2</sub> concentration are a rise in ocean temperature and acidification (i.e., lower pH). Temperature alone is considered to be the “abiotic master factor” as it is known to affect nearly every metabolic process in fishes (Fry, 1971; Brett, 1971). In fact, fishes are known to select different temperatures in order to enhance physiological processes (Sims et al., 2006; Wallman and Bennett, 2006; Di Santo and Bennett, 2011a). As ocean temperature increases as a consequence of climate change, we might expect fish to adjust to the new thermal environment through physiological acclimatization (Somero, 2010; Donelson et al., 2012), adaptation (Angilletta et al., 2004; Baumann and Conover, 2011; Di Santo, 2015), or behavioral thermoregulation (Perry et al., 2005; Greenstein and Pandolfi, 2008).

Similarly to other metabolic processes, swimming performance in fishes is known to be affected by abiotic climate-related factors such as temperature and pH (Chin and Kyne, 2007; Ishimatsu et al., 2008; Pang et al., 2011; Chen et al., 2011). Swimming performance increases with temperature up to a thermal optimum, beyond which performance declines rapidly. As organisms often live close to their thermal optimum, even a slight increase in ambient temperature may drastically reduce the energy available for highly demanding aerobic activities, such as locomotion (Rummer et al., 2014; Di Santo, in review; Brill and Lai, 2015). Locomotor efficiency is key to survival and reproduction in fishes, as swimming is used to migrate daily and seasonally to forage, spawn, and avoid predators. In addition, in light of environmental change, efficient locomotion may also ensure that elasmobranch fishes are able to find suitable refugia. Relocation to more favorable areas assumes that populations

of elasmobranchs will be able to find and move to the new locations, and this assumption should be treated with caution (Chin and Kyne, 2007). The ability (or lack of thereof) to undertake large-scale migrations raises serious concerns especially for less mobile, or philopatric species that tend to remain close to their home areas. When comparing the costs of transport and metabolic rates of a range of elasmobranch and teleost fishes, it becomes apparent that metabolic rates *per se* are not a good indicator to predict the ability of a fish to migrate (Table 6.1). In fact, even though the European eel, *Anguilla Anguilla*, has comparable swimming metabolic rates to the little skate (62.7 vs. 69.5 mgO<sub>2</sub> × kg<sup>-1</sup> × h<sup>-1</sup>), it uses over five times less energy than the little skate to cover the same distance (Table 6.1). These results correspond to observations of activity of these two species in nature. The European eel has a very low cost of transport as a result of the combination of undulatory locomotor mode, a long body length and low oxygen consumption, and can therefore undertake a migration of 6000 km from Europe to the Sargasso Sea in 180 days (van Ginneken et al., 2005). In contrast, the little skate shows high site fidelity (philopatry) and short migratory distances (Di Santo, 2015), despite the fact that the lowest active metabolic rate measured in this species is comparable to that of the European eel.

Even though, generally, teleosts seem to exhibit lower costs of transport when compared to elasmobranchs based on the available comparative data in Table 6.1, it seems that the small body size of the little skate may reduce efficiency of locomotion over long distances and increase overall energy expenditure. In fact, the little skate has some of the highest costs of transport within elasmobranch species tested to date, and it is only surpassed by more active and larger sharks, such as the mako (Table 6.1). In light of these data, it is important to consider cost of transport along with resting and active metabolic rates to improve predictions of whether or not fish species may be able to significantly shift their geographic range.

Ocean warming is already affecting demography, geographic range, and predator timing of populations and species (Murawski, 1993; Walther et al., 2002; Perry et al., 2005; Parmesan, 2006; Dulvy et al., 2008; Chen et al., 2011). Demographic changes include shifts in recruitment, body size, and survival (Pörtner and Farrell, 2008; Genner et al., 2010; Gardner et al., 2011). Geographic shifts include those toward the poles (Walther et al., 2002; Perry et al., 2005; Beaugrand et al., 2008; Chen et al., 2011), and phenological changes include anticipating the timing of spawning and migrations (Farrell et al., 2008; Martins et al., 2011; Eliason et al., 2011), causing a mismatch between prey and predator timing (Raubenheimer et al., 2012). In particular, warming is thought to expand species ranges toward higher latitudes or deeper waters (Walther et al., 2002; Parmesan, 2006; Burrows et al., 2011). Perry et al. (2005) documented a shift in mean depth of the cuckoo ray, *Leucoraja naevus*, with

species moving to deeper water as a response to warming, while [Stebbing et al. \(2002\)](#) showed a correlation between warming of the North Atlantic and migration of warmer water elasmobranch species, such as the sharpnose sevengill *Heptranchias perlo* and big-eye thresher *Alopias superciliosus*, to the Cornish coasts of Great Britain. Some species are highly migratory and may travel across oceans to exploit seasonal productivity events (see [Camhi et al., 2008](#), for review). It is clear that, in order to undertake such large-scale migration toward suitable refugia, elasmobranch fishes should be able to sustain prolonged swimming, and more data are needed to determine migratory capacities.

Compared to viviparous elasmobranchs, oviparous species such as skates have a reduced geographic distribution ([Goodwin et al., 2005](#)). This is thought to occur because skates are typically smaller in size than livebearing elasmobranchs, and size correlates with the ability to maintain wider geographic ranges ([Musick et al., 2004](#)). Additionally, skates have to restrict their ranges to suitable spawning habitats, because embryos are spatially and temporally constrained in the egg case for a prolonged period of time (one or more seasons; [Palm et al., 2011](#); [Di Santo, 2015](#)). As a consequence, although some batoids undertake seasonal latitudinal migrations, some species, like the little skate in the Northwestern Atlantic, only show weak seasonal distribution patterns that consist of short distance movements from coastal and shallow waters to offshore and deeper waters during colder months ([McEachran, 2002](#)). Perhaps because of these spawning and spatial constraints, growth rates and maturation times are different in adjacent populations of little skates from the Gulf of Maine and Georges Bank ([Di Santo, 2015](#)).

In addition, when the effects of increasing temperature and acidification on the costs of the escape response were tested in the little skate by employing a chasing protocol, performance showed a decline even with a modest increase in temperature (3°C) beyond the thermal optimum ([Fig. 6.7](#)). This effect is particularly pronounced in skates from the Gulf of Maine, thus underscoring the importance of comparative studies of locally adapted populations within a species. An additional factor that can affect locomotor performance is acidification, which is known to exacerbate the effect of warming on elasmobranch swimming performance. In fact, increased water acidification reduced the escape performance (intensity of response and aerobic scope) in juvenile little skates from the Gulf of Maine, while a much less pronounced effect was observed in the Georges Bank population ([Fig. 6.7](#)). Even though the increase in temperature and acidification was not lethal in this species, it decreased endurance during the escape response, and prolonged recovery time after exhaustive exercise ([Fig. 6.8](#)), thus reducing the likelihood that the fish will be resilient in changing environment. While low pH increased recovery time in both populations, skates from the Gulf of Maine exhibited elevated metabolic

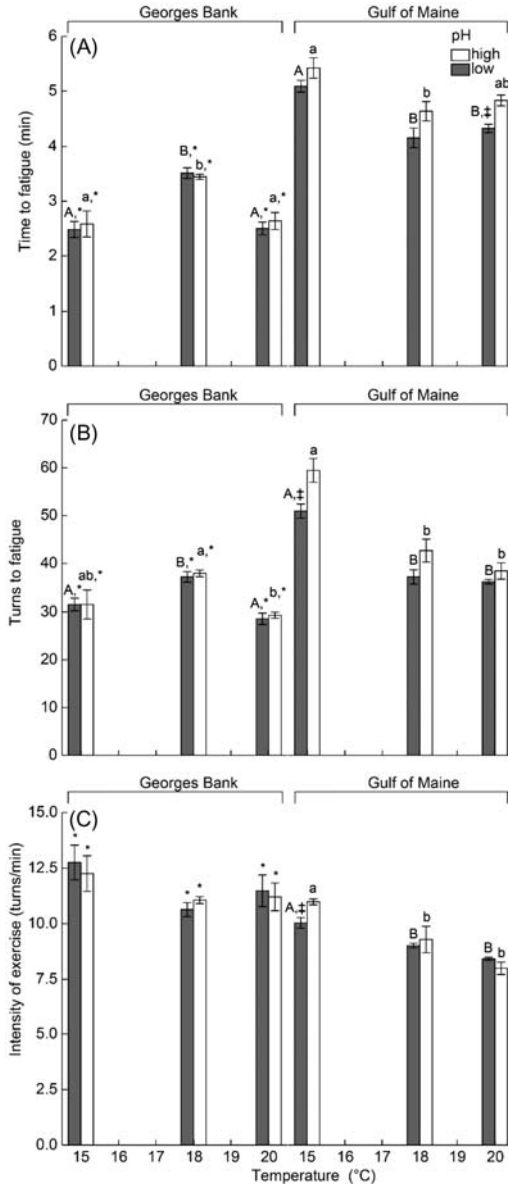


**Figure 6.7.** (A) Time to fatigue, (B) turns to fatigue, (C) intensity of exercise measured in turns per minute (mean  $\pm$  SE) for *Leucoraja erinacea* from the Gulf of Maine ( $n=24$ ) and the Georges Bank ( $n=24$ ) at three temperatures and two pH conditions (*high*=8.1 and *low*=7.7). Different pH levels were controlled as suggested by Riebesell et al. (2010) according to high emission scenarios by year 2100 model RCP 8.5 (IPCC, 2013). Different lower and upper case letters represent significant differences within high and low pH conditions, respectively; double daggers represent significant differences between pH treatment at each temperature; asterisks represent significant differences between populations (Tukey-Kramer MCT;  $\alpha=0.05$ ) (Di Santo, in review).

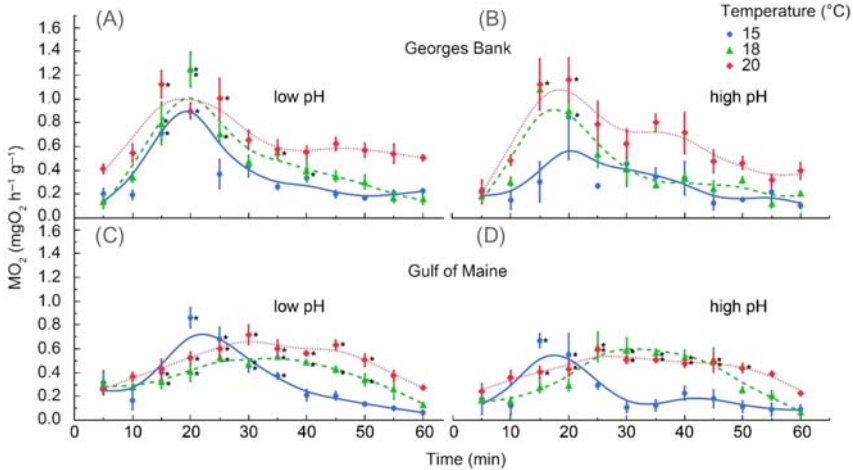


**Figure 6.8.** Post-exhaustion oxygen consumption responses (mean  $\pm$  SE) in two populations (Georges Bank, A and B, and Gulf of Maine, C and D) of juvenile little skate *Leucoraja erinacea* ( $n = 24$  per population) raised in common garden conditions to mimic current and future levels of warming and acidification (*high pH* = 8.1, *low pH* = 7.7). Colors indicate different temperatures. The symbol \* indicates significant difference in mean oxygen consumption between resting metabolic rates (controls) and post-exhaustion metabolic rates (repeated measures ANOVA followed by Dunnett's test,  $p < 0.05$ ) (Di Santo, in review).

rates for as much as double the time as individuals from Georges Bank (Fig. 6.8), making them potentially more vulnerable to ocean acidification.

Whenever migration or dispersal capacities are restricted because of a limited locomotor capacity, or surrounding habitats are unsuitable, climate change is expected to cause widespread extinctions (Dulvy et al., 2008). Because the response to temperature and acidification increase is likely to be species- and age-specific, it is plausible to expect demographic and functional shifts in marine ecosystems (Perry et al., 2005). Local extirpation of ecologically important species, like elasmobranchs, have the potential to destabilize ecosystem functioning. It has been suggested that species with faster generation times will be able to respond more rapidly to environmental changes either through adaptation or by shifting geographic ranges toward more suitable habitats (Somero, 2010). However, elasmobranchs are typically large and even smaller species may grow and mature at a slow rate, making them particularly susceptible to rapid changes in the environment. Until recently, plastic responses were not considered a possible long-term solution to directional change in the environment, but recent studies have proposed that transgenerational acclimation to warming and acidification may increase performance of offspring of fishes exposed to increased

temperature (Ho and Burggren, 2009; Donelson et al., 2011; Grossniklaus et al., 2013). Although a number of studies have examined the effect of ocean warming and acidification on teleost fishes over the past five years (e.g., Checkley et al., 2009; Baumann and Conover, 2011; Baumann et al., 2012; Nilsson et al., 2012), our understanding of the impacts on elasmobranch species is still surprisingly limited. To improve management practices for elasmobranch populations, there is an urgent need for implementation of multistressor studies on different life stages and on individuals sampled at different locations. This will allow us to identify critical life stages for survival, as well as the potential for acclimation and/or adaptation in swimming performance when directional environmental change occurs (Melzner et al., 2009; Checkley et al., 2009; Baumann and Conover, 2011; Baumann et al., 2012; Nilsson et al., 2012). Multistressor studies on different life stages and locally adapted populations may also allow us to understand the mechanisms underlying resilience to warming and acidification and ultimately can aid in determining “winning and losing” elasmobranch phenotypes under a changing climate.

## 8. CONCLUSIONS

Despite considerable progress toward understanding elasmobranch locomotion in recent years, there is still much to be done with some surprising gaps remaining. In particular, there are relatively few data on elasmobranch locomotor energetics and batoid swimming energetics in particular, for which data are only available for one small skate species (Table 6.1). Active metabolic rates of pelagic sharks are certainly extremely challenging to measure directly, and controlled studies in a laboratory flume setting will be difficult to achieve given the complications of swimming large sharks in the confined space of a flume working section. Surrogate and indirect metrics such as heart rate do not provide a complete picture of the cost of transport, and it is likely that values of active metabolic rates for many shark species will remain largely inferential for some time to come.

But even fundamental kinematic analyses of body and tail deformation during swimming are limited to a few species, and three-dimensional data are available for even fewer and mostly smaller species. A much broader quantitative study of locomotor kinematics in three-dimensions is key to understanding the diversity of locomotor modes and the relation between body shape and bending patterns of the body and tail during swimming and maneuvering. The remarkable diversity of elasmobranch shape and internal structure is not reflected in functional studies, which to date have focused on

a very limited subset of diversity. A key challenge for the future is to extend current work on locomotor biomechanics to encompass a variety of species of different habits and forms.

### ACKNOWLEDGMENTS

This work was supported by ONR-MURI Grant N000141410533 monitored by Dr. Bob Brizzolara, ONR grant N00014-09-1-0352 monitored by Dr. Tom McKenna, and by National Science Foundation grants EFRI-0938043 and CDI 0941674. Many thanks to all our collaborators for their assistance and efforts to better understand elasmobranch locomotion over the years.

### REFERENCES

- Affleck, R. J. (1950). Some points in the function, development, and evolution of the tail in fishes. *Proc. Zool. Soc. Lond.* **120**, 349–368.
- Allan, B. J., Domenici, P., McCormick, M. I., Watson, S.-A. and Munday, P. L. (2013). Elevated CO<sub>2</sub> affects predator-prey interactions through altered performance. *PLoS One* **8**, e58520.
- Anderson, E. J., McGillis, W. and Grosenbaugh, M. A. (2001). The boundary layer of swimming fish. *J. Exp. Biol.* **204**, 81–102.
- Angilletta, M. J., Oufiero, C. E. and Sears, M. W. (2004). Thermal adaptation of maternal and embryonic phenotypes in a geographically widespread ectotherm animals and environments. In *Proceedings of the Third International Conference of Comparative Physiology and Biochemistry*, KwaZulu-Natal, South Africa, 7–13 August 2004, vol. 1275. Elsevier, pp. 258–266.
- Baumann, H. and Conover, D. O. (2011). Adaptation to climate change: contrasting patterns of thermal-reaction-norm evolution in Pacific versus Atlantic silversides. *Proc. R. Soc. B Biol. Sci.* **278**, 2265–2273.
- Baumann, H., Talmage, S. C. and Gobler, C. J. (2012). Reduced early life growth and survival in a fish in direct response to increased carbon dioxide. *Nat. Clim. Change* **2**, 38–41.
- Beaugrand, G., Edwards, M., Brander, K., Luczak, C. and Ibanez, F. (2008). Causes and projections of abrupt climate-driven ecosystem shifts in the North Atlantic. *Ecol. Lett.* **11**, 1157–1168.
- Bechert, D. W. and Hage, W. (2007). Drag reduction with riblets in nature and engineering. In *Flow Phenomena in Nature. Volume 2. Inspiration, Learning, and Application*, vol. 2 (ed. R. Liebe), pp. 457–469. Southampton, UK: WIT Press.
- Bechert, D. W., Bartenwerfer, M., Hoppe, G. and Reif, W. E. (1986). *Drag reduction mechanisms derived from shark skin*. *Proc. 15th Int. Council of Aeronautical Sciences Congress*: London, UK, 7–12 September vol. 2: 1044–1068, paper no. ICAS-86-1.8.3. *AIAA*.
- Bernal, D., Dickson, K. A., Shadwick, R. E. and Graham, J. B. (2001). Analysis of the evolutionary convergence for high performance swimming in lamnid sharks and tunas. *Comp. Biochem. Physiol. A* **129**, 695–726.
- Bernal, D., Donley, J. M., Shadwick, R. E. and Syme, D. A. (2005). Mammal-like muscles power swimming in a cold-water shark. *Nature* **437**, 1349–1352.
- Bernal, D., Sepulveda, C., Mathieu-Costello, O. and Graham, J. B. (2003a). Comparative studies of high performance swimming in sharks I. Red muscle morphometrics, vascularization and ultrastructure. *J. Exp. Biol.* **206**, 2831–2843.

- Bernal, D., Smith, D., Lopez, G., Weitz, D., Grimminger, T., Dickson, K. A., et al. (2003b). Comparative studies of high performance swimming in sharks II. Metabolic biochemistry of locomotor and myocardial muscle in endothermic and ectothermic sharks. *J. Exp. Biol.* **206**, 2845–2857.
- Bernal, D., Sepulveda, C., Musyl, M. and Brill, R. (2009). The eco-physiology of swimming and movement patterns of tunas, billfishes, and large pelagic sharks. In *Fish locomotion—an etho-ecological Perspective* (eds. P. Domenici and B. G. Kapoor), pp. 436–483. Enfield, NH: Science Publishers.
- Bernal, D., Carlson, J. K., Goldman, K. J. and Lowe, C. G. (2012). *Energetics, Metabolism, and Endothermy in Sharks and Rays: Biology of Sharks and Their Relatives* (second ed.). Boca Raton, FL: CRC Press.
- Binning, S. A., Roche, D. G. and Layton, C. (2013). Ectoparasites increase swimming costs in a coral reef fish. *Biol. Lett.* **9**, 20120927.
- Blevins, E. and Lauder, G. V. (2012). Rajiform locomotion: three-dimensional kinematics of the pectoral fin surface during swimming by the freshwater stingray *Potamotrygon orbignyi*. *J. Exp. Biol.* **215**, 3231–3241.
- Blevins, E. L. and Lauder, G. V. (2013). Swimming near the substrate: a simple robotic model of stingray locomotion. *Bioinsp. Biomimet.* **8**, 016005.
- Bone, Q. (1966). On the function of the two types of myotomal muscle fibre in elasmobranch fish. *J. Mar. Biol. Ass. U.K.* **46**, 321–349.
- Bone, Q. (1978). Locomotor muscle. In *Fish Physiology: Locomotion*, vol. 7 (eds. W. S. Hoar and D. J. Randall), pp. 1–100. New York, NY: Academic Press.
- Bone, Q. (1988). Muscles and locomotion. In *Physiology of Elasmobranch Fishes* (ed. T. J. Shuttleworth), pp. 99–141. Berlin: Springer Verlag.
- Bone, Q. (1999). Muscular system: microscopical anatomy, physiology, and biochemistry of elasmobranch muscle fibers. In *Sharks, Skates, and Rays: The Biology of Elasmobranch Fishes* (ed. W. C. Hamlett), pp. 115–143. Baltimore, MD: Johns Hopkins University Press.
- Bone, Q., Kiceniuk, J. and Jones, D. R. (1978). On the role of the different fibre types in fish myotomes at intermediate swimming speeds. *Fish. Bull.* **76**, 691–699.
- Bonfil, R., Mejer, M., Scholl, M. C., Johnson, R., O'Brien, S., Oosthuizen, H., et al. (2005). Transoceanic migration, spatial dynamics, and population linkages of white sharks. *Science* **310**, 100–103.
- Borazjani, I. and Daghooghi, M. (2013). The fish tail motion forms an attached leading edge vortex. *Proc. R. Soc. Biol. Sci.* **280**, 20122071.
- Breder, C. M. (1926). The locomotion of fishes. *Zool. N. Y.* **4**, 159–256.
- Brett, J. and Blackburn, J. (1978). Metabolic rate and energy expenditure of the spiny dogfish, *Squalus acanthias*. *J. Fish. Bd. Can.* **35**, 816–821.
- Brett, J. R. (1971). Energetic responses of salmon to temperature. A study of some thermal relations in the physiology and freshwater ecology of sockeye salmon (*Oncorhynchus nerka*). *Am. Zool.* **11**, 99–113.
- Brill, R. W., Lai, N. C., 2015. Elasmobranch cardiovascular system. In *Physiology of Elasmobranch Fishes: Internal Processes*, vol. 34B (eds. R. E. Shadwick, A. P. Farrell and C. Brauner).
- Burrows, M. T., Schoeman, D. S., Buckley, L. B., Moore, P., Poloczanska, E. S., Brander, K. M., et al. (2011). The pace of shifting climate in marine and terrestrial ecosystems. *Science* **334**, 652–655.
- Camhi, M. D., Fordham, S. V. and Fowler, S. L. (2008). Domestic and international management for pelagic sharks. In *Sharks of the Open Ocean: Biology, Fisheries and Conservation* (eds. M. D. Camhi, E. K. Pikitch and E. A. Babcock). Oxford, UK: Blackwell Publishing Ltd.

- Carlson, J. K. and Parsons, G. R. (2001). The effects of hypoxia on three sympatric shark species: physiological and behavioral responses. *Environ. Biol. Fish.* **61**, 427–433.
- Carlson, J. K., Palmer, C. L. and Parsons, G. R. (1999). Oxygen consumption rate and swimming efficiency of the blacknose shark, *Carcharhinus acronotus*. *Copeia* **1999**, 34–39.
- Checkley, D. M., Dickson, A. G., Takahashi, M., Radich, J. A., Eisenkolb, N. and Asch, R. (2009). Elevated CO<sub>2</sub> enhances otolith growth in young fish. *Science* **324**, 1683–1683.
- Chen, I.-C., Hill, J. K., Ohlemüller, R., Roy, D. B. and Thomas, C. D. (2011). Rapid range shifts of species associated with high levels of climate warming. *Science* **333**, 1024–1026.
- Chin, A., Kyne, P. M., 2007. Vulnerability of chondrichthyan fishes of the Great Barrier Reef to climate change. In *Climate Change and the Great Barrier Reef* (eds. J. E. Johnson and P. A. Marshall), pp. 393–425. Townsville, Australia: Great Barrier Reef Marine Park Authority and Australian Greenhouse Office.
- Clark, E. (1963). Massive aggregations of large rays and sharks in and near Sarasota, Florida. *Zoologica* **48**, 61–66.
- Clark, T. D., Sandblom, E. and Jutfelt, F. (2013). Aerobic scope measurements of fishes in an era of climate change: respirometry, relevance and recommendations. *J. Exp. Biol.* **216**, 2771–2782.
- Cutts, C. J., Metcalfe, N. B. and Taylor, A. C. (2002). Juvenile Atlantic salmon (*Salmo salar*) with relatively high standard metabolic rates have small metabolic scopes. *Funct. Ecol.* **16**, 73–78.
- Daniel, T. L. (1988). Forward flapping flight from flexible fins. *Can. J. Zool.* **66**, 630–638.
- Dean, B. and Bhushan, B. (2010). Shark-skin surfaces for fluid-drag reduction in turbulent flow: a review. *Phil. Trans. R. Soc. A Math. Phys. Eng. Sci.* **368**, 4775–4806.
- Dean, M. N. and Summers, A. P. (2006). Mineralized cartilage in the skeleton of chondrichthyan fishes. *Zoology* **109**, 164–168.
- Dean, M. N., Mull, C. G., Gorb, S. N. and Summers, A. P. (2009). Ontogeny of the tessellated skeleton: insight from the skeletal growth of the round stingray *Urolophus halleri*. *J. Anat.* **215**, 227–239.
- Dewar, H. and Graham, J. (1994). Studies of tropical tuna swimming performance in a large water tunnel—energetics. *J. Exp. Biol.* **192**, 13–31.
- Di Santo, V. (2015). Ocean acidification exacerbates the impacts of global warming on embryonic little skate, *Leucoraja erinacea* (Mitchill). *J. Exp. Marine Biol. Ecol.* **463**, 72–78.
- Di Santo, V. and Bennett, W. A. (2011a). Is post-feeding thermotaxis advantageous in elasmobranch fishes? *J. Fish Biol.* **78**, 195–207.
- Di Santo, V. and Bennett, W. A. (2011b). Effect of rapid temperature change on resting routine metabolic rates of two benthic elasmobranchs. *Fish Physiol. Biochem.* **37**, 1–6.
- Domenici, P., Standen, E. M. and Levine, R. P. (2004). Escape manoeuvres in the spiny dogfish (*Squalus acanthias*). *J. Exp. Biol.* **207**, 2339–2349.
- Donelson, J. M., Munday, P. L., McCormick, M. I. and Nilsson, G. E. (2011). Acclimation to predicted ocean warming through developmental plasticity in a tropical reef fish. *Glob. Change Biol.* **17**, 1712–1719.
- Donelson, J. M., Munday, P. L., McCormick, M. I. and Pitcher, C. R. (2012). Rapid transgenerational acclimation of a tropical reef fish to climate change. *Nat. Clim. Change* **2**, 30–32.
- Donley, J. and Shadwick, R. (2003). Steady swimming muscle dynamics in the leopard shark *Triakis semifasciata*. *J. Exp. Biol.* **206**, 1117–1126.
- Donley, J., Sepulveda, C., Konstantinidis, P., Gemballa, S. and Shadwick, R. (2004). Convergent evolution in mechanical design of lamnid sharks and tunas. *Nature* **429**, 61–65.
- Drucker, E. G. and Lauder, G. V. (1999). Locomotor forces on a swimming fish: three-dimensional vortex wake dynamics quantified using digital particle image velocimetry. *J. Exp. Biol.* **202**, 2393–2412.

- Drucker, E. G. and Lauder, G. V. (2001). Locomotor function of the dorsal fin in teleost fishes: experimental analysis of wake forces in sunfish. *J. Exp. Biol.* **204**, 2943–2958.
- Dulvy, N. K., Rogers, S. I., Jennings, S., Stelzenmüller, V., Dye, S. R. and Skjoldal, H. R. (2008). Climate change and deepening of the North Sea fish assemblage: a biotic indicator of warming seas. *J. Appl. Ecol.* **45**, 1029–1039.
- Eliason, E. J., Clark, T. D., Hague, M. J., Hanson, L. M., Gallagher, Z. S., Jeffries, K. M., et al. (2011). Differences in thermal tolerance among sockeye salmon populations. *Science* **332**, 109–112.
- Ezcurra, J. M., Lowe, C. G., Mollet, H. F., Ferry, L. A. and O'Sullivan, J. B. (2012). Captive feeding and growth of young-of-the-year white sharks, *Carcharodon carcharias*, at the Monterey Bay Aquarium. In *Global Perspectives on the Biology and Life History of the White Shark* (ed. M. L. Domeier), pp. 3–15. Boca Raton, FL: CRC Press.
- Farrell, A. P., Hinch, S. G., Cooke, S. J., Patterson, D. A., Crossin, G. T., Lapointe, M., et al. (2008). Pacific salmon in hot water: applying aerobic scope models and biotelemetry to predict the success of spawning migrations. *Physiol. Biochem. Zool.* **81**, 697–709.
- Farrell, A. P., Eliason, E. J., Sandblom, E. and Clark, T. D. (2009). Fish cardiorespiratory physiology in an era of climate change. *Can. J. Zool.* **87**, 835–851.
- Ferry, L. A. and Lauder, G. V. (1996). Heterocercal tail function in leopard sharks: a three-dimensional kinematic analysis of two models. *J. Exp. Biol.* **199**, 2253–2268.
- Ferry-Graham, L. A. and Gibb, A. C. (2001). Comparison of fasting and postfeeding metabolic rates in a sedentary shark, *Cephaloscyllium ventriosum*. *Copeia* **2001**, 1108–1113.
- Fish, F. E. and Shannahan, L. D. (2000). The role of the pectoral fins in body trim of sharks. *J. Fish. Biol.* **56**, 1062–1073.
- Flammang, B. E. (2010). Functional morphology of the radialis muscle in shark tails. *J. Morphol.* **271**, 340–352.
- Flammang, B. E., Lauder, G. V., Troolin, D. R. and Strand, T. (2011). Volumetric imaging of shark tail hydrodynamics reveals a three-dimensional dual-ring vortex wake structure. *Proc. R. Soc. Lond. B* **278**, 3670–3678.
- Fontanella, J. E., Fish, F. E., Barchi, E. I., Campbell-Malone, R., Nichols, R. H., DiNenno, N. K., et al. (2013). Two- and three-dimensional geometries of batoids in relation to locomotor mode. *J. Exp. Mar. Biol. Ecol.* **446**, 273–281.
- Fry, F. E. J. (1947). *Effects of the Environment on Animal Activity*. Toronto: University of Toronto Press.
- Fry, F. (1971). The effect of environmental factors on the physiology of fish. In *Fish Physiology: Environmental Relations and Behavior*, vol. 6 (eds. W. S. Hoar and D. J. Randall), pp. 1–98. New York: Academic Press.
- Gardner, J. L., Peters, A., Kearney, M. R., Joseph, L. and Heinsohn, R. (2011). Declining body size: a third universal response to warming? *Trends Ecol. Evol.* **26**, 285–291.
- Genner, M. J., Sims, D. W., Southward, A. J., Budd, G. C., Masterson, P., Mchugh, M., et al. (2010). Body size-dependent responses of a marine fish assemblage to climate change and fishing over a century-long scale. *Glob. Change Biol.* **16**, 517–527.
- Gleiss, A. C., Dale, J. J., Holland, K. N. and Wilson, R. P. (2010). Accelerating estimates of activity-specific metabolic rate in fishes: testing the applicability of acceleration dataloggers. *J. Exp. Mar. Biol. Ecol.* **385**, 85–91.
- Goodwin, N. B., Dulvy, N. K. and Reynolds, J. D. (2005). Macroecology of live-bearing in fishes: latitudinal and depth range comparisons with egg-laying relatives. *Oikos* **110**, 209–218.
- Graham, J. B., DeWar, H., Lai, N., Lowell, W. R. and Arce, S. M. (1990). Aspects of shark swimming performance determined using a large water tunnel. *J. Exp. Biol.* **151**, 175–192.
- Graham, J. B., Dewar, H., Lai, N. C., Korsmeyer, K. E., Fields, P. A., Knower, T., et al. (1994). Swimming physiology of pelagic fishes. In *Mechanics and Physiology of Animal Swimming* (eds. L. Maddock, Q. Bone and J. M. V. Rayner), pp. 63–74. Cambridge: Cambridge University Press.

- Graham, R. T., Witt, M. J., Castellanos, D. W., Remolina, F., Maxwell, S., Godley, B. J., et al. (2012). Satellite tracking of manta rays highlights challenges to their conservation. *PLoS One* **7**, e36834.
- Greenstein, B. J. and Pandolfi, J. M. (2008). Escaping the heat: range shifts of reef coral taxa in coastal Western Australia. *Glob. Change Biol.* **14**, 513–528.
- Grossniklaus, U., Kelly, W. G., Ferguson-Smith, A. C., Pembrey, M. and Lindquist, S. (2013). Transgenerational epigenetic inheritance: how important is it? *Nat. Rev. Genet.* **14**, 228–235.
- Ho, D. H. and Burggren, W. W. (2009). Epigenetics and transgenerational transfer: a physiological perspective. *J. Exp. Biol.* **213**, 3–16.
- IPCC (2013). *Climate Change: The Assessment Reports of the Intergovernmental Panel on Climate Change*. Cambridge, UK: Cambridge University Press.
- Irschick, D. and Hammerschlag, N. (2014a). A new metric for measuring condition in large predatory sharks. *J. Fish. Biol.* **85**, 917–926.
- Irschick, D. J. and Hammerschlag, N. (2014b). Morphological scaling of body form in four shark species differing in ecology and life history. *Biol. J. Linn. Soc.* **114**, 126–135.
- Ishimatsu, A., Hayashi, M. and Kikkawa, T. (2008). Fishes in high-CO<sub>2</sub>, acidified oceans. *Marine Ecol. Prog. Ser.* **373**, 295–302.
- Jorgensen, S. J., Reeb, C. A., Chapple, T. K., Anderson, S., Perle, C., Van Sommeran, S. R., et al. (2010). Philopatry and migration of pacific white sharks. *Proc. R. Soc. B Biol. Sci.* **277**, 679–688.
- Kajiura, S. M., Forni, J. and Summers, A. (2003). Maneuvering in juvenile carcharhinid and sphyrnid sharks: the role of the hammerhead shark cephalofoil. *Zoology* **106**, 19–28.
- Kemp, N. E. (1999). Integumentary system and teeth. In *Sharks, Skates, and Rays: The Biology of Elasmobranch Fishes* (ed. W. C. Hamlett), pp. 43–68. Baltimore, MD: Johns Hopkins University Press.
- Klausewitz, W. (1964). Der Locomotionsmodus der Flugelrochen (Myliobatoidei). *Zool. Anz.* **173**, 111–120.
- Koester, D. M. and Spirito, C. P. (2003). Punting: an unusual mode of locomotion in the little skate, *Leucoraja erinacea* (Chondrichthyes: Rajidae). *Copeia* **2003**, 553–561.
- Korsmeyer, K., Steffensen, J. and Herskin, J. (2002). Energetics of median and paired fin swimming, body and caudal fin swimming, and gait transition in parrotfish (*Scarus schlegelii*) and triggerfish (*Rhinecanthus aculeatus*). *J. Exp. Biol.* **205**, 1253–1263.
- Lang, A. W., Motta, P., Hidalgo, P. and Westcott, M. (2008). Bristled shark skin: a microgeometry for boundary layer control? *Bioinsp. Biomimet.* **3**, 046005.
- Lang, A. W., Bradshaw, M. T., Smith, J. A., Wheelus, J. N., Motta, P. J., Habegger, M. L., et al. (2014). Movable shark scales act as a passive dynamic micro-roughness to control flow separation. *Bioinsp. Biomimet.* **9**, 036017.
- Lauder, G. V. (2006). Locomotion. In *The Physiology of Fishes* (eds. D. H. Evans and J. B. Claiborne), third ed., pp. 3–46. Boca Raton, FL: CRC Press.
- Lauder, G. V. (2015). Fish locomotion: recent advances and new directions. *Annu. Rev. Marine Sci.* **7**, 521–545.
- Lauder, G. V., Anderson, E. J., Tangorra, J. and Madden, P. G. A. (2007). Fish biorobotics: kinematics and hydrodynamics of self-propulsion. *J. Exp. Biol.* **210**, 2767–2780.
- Lauder, G. V., Lim, J., Shelton, R., Witt, C., Anderson, E. J. and Tangorra, J. (2011). Robotic models for studying undulatory locomotion in fishes. *Marine Tech. Soc. J.* **45**, 41–55.
- Lauder, G. V., Flammang, B. E. and Alben, S. (2012). Passive robotic models of propulsion by the bodies and caudal fins of fish. *Int. Comp. Biol.* **52**, 576–587.
- Liem, K. F., Bemis, W. E., Walker, W. F. and Grande, L. (2001). *Functional Anatomy of the Vertebrates. An Evolutionary Perspective* (third ed.). Fort Worth, TX: Harcourt College Publishers.

- Lindsey, C. C. (1978). Form, function, and locomotory habits in fish. In *Fish Physiology: Locomotion*, vol. 7 (eds. W. S. Hoar and D. J. Randall), pp. 1–100. New York, NY: Academic Press.
- Liu, X., Dean, M. N., Summers, A. P. and Earthman, J. C. (2010). Composite model of the shark's skeleton in bending: a novel architecture for biomimetic design of functional compression bias. *Mater. Sci. Eng. C* **30**, 1077–1084.
- Long, J., Koob, T., Irving, K., Combie, K., Engel, V., Livingston, N., et al. (2006). Biomimetic evolutionary analysis: testing the adaptive value of vertebrate tail stiffness in autonomous swimming robots. *J. Exp. Biol.* **209**, 4732–4746.
- Long, J., Koob, T. J., Schaefer, J., Summers, A., Bantilan, K., Grotmol, S., et al. (2011). Inspired by sharks: a biomimetic skeleton for the flapping, propulsive tail of an aquatic robot. *Marine Tech. Soc. J.* **45**, 119–129.
- Lowe, C. (1996). Kinematics and critical swimming speed of juvenile scalloped hammerhead sharks. *J. Exp. Biol.* **199**, 2605–2610.
- Lowe, C. G. (2002). Bioenergetics of free-ranging juvenile scalloped hammerhead sharks (*Sphyrna lewini*) in Kāne'ohe Bay, O'ahu, HI. *J. Exp. Mar. Biol. Ecol.* **278**, 141–156.
- Macesic, L. J. and Kajiura, S. M. (2010). Comparative punting kinematics and pelvic fin musculature of benthic batoids. *J. Morphol.* **271**, 1219–1228.
- Macesic, L. J. and Summers, A. P. (2012). Flexural stiffness and composition of the batoid propterygium as predictors of punting ability. *J. Exp. Biol.* **215**, 2003–2012.
- Macesic, L. J., Mulvaney, D. and Blevins, E. L. (2013). Synchronized swimming: coordination of pelvic and pectoral fins during augmented punting by the freshwater stingray *Potamotrygon orbignyi*. *Zoology* **116**, 144–150.
- Maia, A. and Wilga, C. A. (2013a). Function of dorsal fins in bamboo shark during steady swimming. *Zoology* **116**, 224–231.
- Maia, A. and Wilga, C. D. (2013b). Anatomy and muscle activity of the dorsal fins in bamboo sharks and spiny dogfish during turning maneuvers. *J. Morphol.* **274**, 1288–1298.
- Maia, A., Wilga, C. D. and Lauder, G. V. (2012). Biomechanics of locomotion in sharks, rays and chimeras. In *Biology of Sharks and Their Relatives* (eds. J. C. Carrier, J. A. Musick and M. R. Heithaus), second ed., pp. 125–151. Boca Raton, FL: CRC Press.
- Martins, E. G., Hinch, S. G., Patterson, D. A., Hague, M. J., Cooke, S. J., Miller, K. M., et al. (2011). Effects of river temperature and climate warming on stock-specific survival of adult migrating Fraser River sockeye salmon (*Oncorhynchus nerka*). *Glob. Change Biol.* **17**, 99–114.
- McEachran, J. D. (2002). Skates. family Rajidae. In *Bigelow and Schroeder's Fishes of the Gulf of Maine* (eds. B. B. Collette and G. Klein-Macphée), third ed., pp. 60–75. Washington, D.C.: Smithsonian Institution Press.
- Meloni, C. J., Cech, J. J., Jr., Katzman, S. M. and Gatten, R. E., Jr. (2002). Effect of brackish salinities on oxygen consumption of bat rays (*Myliobatis californica*). *Copeia* **2002**, 462–465.
- Melzner, F., Gutowska, M. A., Langenbuch, M., Dupont, S., Lucassen, M., Thorndyke, M. C., et al. (2009). Physiological basis for high CO<sub>2</sub> tolerance in marine ectothermic animals: pre-adaptation through lifestyle and ontogeny? *Biogeosciences* **6**, 2313–2331.
- Moored, K. W., Dewey, P. A., Leftwich, M., Bart-Smith, H. and Smits, A. (2011a). Bioinspired propulsion mechanisms based on manta ray locomotion. *Marine Tech. Soc. J.* **45**, 110–118.
- Moored, K. W., Fish, F., Kemp, T. H. and Bart-Smith, H. (2011b). Batoid fishes: inspiration for the next generation of underwater robots. *Marine Tech. Soc. J.* **45**, 99–109.
- Motta, P., Habegger, M. L., Lang, A., Hueter, R. and Davis, J. (2012). Scale morphology and flexibility in the shortfin mako *Isurus oxyrinchus* and the blacktip shark *Carcharhinus limbatus*. *J. Morphol.* **273**, 1096–1110.

- Motta, P. J. (1977). Anatomy and functional morphology of dermal collagen fibres in sharks. *Copeia* **1977**, 454–464.
- Murawski, S. A. (1993). Climate change and marine fish distributions: forecasting from historical analogy. *Trans. Am. Fish. Soc.* **122**, 647–658.
- Musick, J. A., Harbin, M. M. and Compagno, L. J. (2004). Historical zoogeography of the Selachii. In *Biology of Sharks and Their Relatives* (eds. J. Carrier and J. Musick), pp. 33–78. Boca Raton, FL: CRC Press.
- Nilsson, G. E., Dixon, D. L., Domenici, P., McCormick, M. I., Sørensen, C., Watson, S.-A., et al. (2012). Near-future carbon dioxide levels alter fish behaviour by interfering with neurotransmitter function. *Nat. Clim. Change* **2**, 201–204.
- Oeffner, J. and Lauder, G. V. (2012). The hydrodynamic function of shark skin and two biomimetic applications. *J. Exp. Biol.* **215**, 785–795.
- Palm, B. D., Koester, D. M., Driggers, W. B. and Sulikowski, J. A. (2011). Seasonal variation in fecundity, egg case viability, gestation, and neonate size for little skates, *Leucoraja erinacea*, in the Gulf of Maine. *Environ. Biol. Fish.* **92**, 585–589.
- Pang, X., Cao, Z.-D. and Fu, S.-J. (2011). The effects of temperature on metabolic interaction between digestion and locomotion in juveniles of three cyprinid fish (*Carassius auratus*, *Cyprinus carpio* and *Spinibarbus sinensis*). *Comp. Biochem. Physiol. Part A Mol. Integ. Physiol.* **159**, 253–260.
- Parmesan, C. (2006). Ecological and evolutionary responses to recent climate change. *Annu. Rev. Ecol. Evol. Syst.* **37**, 637–669.
- Parson, J. M., Fish, F. E. and Nicastro, A. J. (2011). Turning performance of batoids: limitations of a rigid body. *J. Exp. Mar. Biol. Ecol.* **402**, 12–18.
- Parsons, G. and Carlson, J. (1998). Physiological and behavioral responses to hypoxia in the bonnethead shark, *Sphyrna tiburo*: routine swimming and respiratory regulation. *Fish Physiol. Biochem.* **19**, 189–196.
- Parsons, G. R. (1990). Metabolism and swimming efficiency of the bonnethead shark, *Sphyrna tiburo*. *Mar. Biol.* **104**, 363–367.
- Perry, A. L., Low, P. J., Ellis, J. R. and Reynolds, J. D. (2005). Climate change and distribution shifts in marine fishes. *Science* **308**, 1912–1915.
- Piiper, J., Meyer, M., Worth, H. and Willmer, H. (1977). Respiration and circulation during swimming activity in the dogfish *Scyliorhinus stellaris*. *Respir. Physiol.* **30**, 221–239.
- Porter, M. E. and Long, J. H. (2010). Vertebrae in compression: mechanical behavior of arches and centra in the gray smooth-hound shark (*Mustelus californicus*). *J. Morphol.* **271**, 366–375.
- Porter, M. E., Beltran, J. L., Koob, T. J. and Summers, A. P. (2006). Material properties and biochemical composition of mineralized vertebral cartilage in seven elasmobranch species (Chondrichthyes). *J. Exp. Biol.* **209**, 2920–2928.
- Porter, M. E., Koob, T. J. and Summers, A. P. (2007). The contribution of mineral to the material properties of vertebral cartilage from the smooth-hound shark *Mustelus californicus*. *J. Exp. Biol.* **210**, 3319–3327.
- Porter, M. E., Roque, C. M. and Long, J. H. (2009). Turning maneuvers in sharks: predicting body curvature from axial morphology. *J. Morphol.* **270**, 954–965.
- Porter, M. E., Roque, C. M. and Long, J. H., Jr. (2011). Swimming fundamentals: turning performance of leopard sharks (*Triakis semifasciata*) is predicted by body shape and postural reconfiguration. *Zoology* **114**, 348–359.
- Porter, M. E., Diaz, C., Jr, Sturm, J. J., Grotmol, S., Summers, A. P. and Long, J. H., Jr (2014). Built for speed: strain in the cartilaginous vertebral columns of sharks. *Zoology* **117**, 19–27.
- Pörtner, H. O. and Farrell, A. P. (2008). Physiology and climate change. *Science* **322**, 690–692.
- Quinn, D. B., Lauder, G. V. and Smits, A. J. (2014a). Flexible propulsors in ground effect. *Bioinsp. Biomimet.* **9**, 1–9.

- Quinn, D. B., Moored, K. W., Dewey, P. A. and Smits, A. J. (2014b). Unsteady propulsion near a solid boundary. *J. Fluid Mech.* **742**, 152–170.
- Raubenheimer, D., Simpson, S. J. and Tait, A. H. (2012). Match and mismatch: conservation physiology, nutritional ecology and the timescales of biological adaptation. *Phil. Trans. R. Soc. B* **367**, 1628–1646.
- Rayner, J. M. V. (1991). On the aerodynamics of animal flight in ground effect. *Phil. Trans. R. Soc. Lond. B* **334**, 119–128.
- Reif, W. (1982). Morphogenesis and function of the squamation in sharks. *Neues J. Geol. Paläon. Abh.* **164**, 172–183.
- Reif, W.-E. (1985). Squamation and ecology of sharks. *Courier Forsch.-Inst. Senckenberg* **78**, 1–255.
- Riebesell, U., Fabry, V. J., Hansson, L. and Gattuso, J. P. (2010). *Guide to Best Practices for Ocean Acidification Research and Data Reporting*. Luxembourg: Publications Office of the European Union.
- Roche, D. G., Binning, S. A., Bosiger, Y., Johansen, J. L. and Rummer, J. L. (2013). Finding the best estimates of metabolic rates in a coral reef fish. *J. Exp. Biol.* **216**, 2103–2110.
- Rosenberger, L. (2001). Pectoral fin locomotion in batoid fishes: undulation *versus* oscillation. *J. Exp. Biol.* **204**, 379–394.
- Rosenberger, L. and Westneat, M. W. (1999). Functional morphology of undulatory pectoral fin locomotion in the stingray *Taeniura lymma* (Chondrichthyes: Dasyatidae). *J. Exp. Biol.* **202**, 3523–3539.
- Rummer, J. L., Couturier, C. S., Stecyk, J. A. W., Gardiner, N. M., Kinch, J. P., Nilsson, G. E., et al. (2014). Life on the edge: thermal optima for aerobic scope of equatorial reef fishes are close to current day temperatures. *Glob. Change Biol.* **20**, 1055–1066.
- Scharold, J. and Gruber, S. H. (1991). Telemetered heart rate as a measure of metabolic rate in the lemon shark, *Negaprion brevirostris*. *Copeia* **1991**, 942–953.
- Scharold, J., Lai, N., Lowell, W. and Graham, J. (1988). Metabolic rate, heart rate, and tailbeat frequency during sustained swimming in the leopard shark *Triakis semifasciata*. *Exp. Biol.* **48**, 223–230.
- Seamone, S., Blaine, T. and Higham, T. E. (2014). Sharks modulate their escape behavior in response to predator size, speed and approach orientation. *Zoology* **117**, 377–382.
- Sepulveda, C. A., Kohin, S., Chan, C., Vetter, R. and Graham, J. (2004). Movement patterns, depth preferences, and stomach temperatures of free-swimming juvenile mako sharks, *Isurus oxyrinchus*, in the Southern California Bight. *Mar. Biol.* **145**, 191–199.
- Sepulveda, C. A., Wegner, N. C., Bernal, D. and Graham, J. B. (2005). The red muscle morphology of the thresher sharks (family Alopiidae). *J. Exp. Biol.* **208**, 4255–4261.
- Sepulveda, C. A., Graham, J. and Bernal, D. (2007). Aerobic metabolic rates of swimming juvenile mako sharks, *Isurus oxyrinchus*. *Mar. Biol.* **152**, 1087–1094.
- Shadwick, R. (2005). How tunas and lamnid sharks swim: an evolutionary convergence. *Am. Sci.* **93**, 524–531.
- Shadwick, R. and Gemballa, S. (2006). Structure, kinematics, and muscle dynamics in undulatory swimming. In *Fish Physiology: Fish Biomechanics*, vol. 23 (eds. R. E. Shadwick and G. V. Lauder), pp. 241–280. San Diego, CA: Academic Press.
- Shadwick, R. E. and Goldbogen, J. A. (2012). Muscle function and swimming in sharks. *J. Fish. Biol.* **80**, 1904–1939.
- Shadwick, R. E. and Lauder, G. V. (2006). *Fish Physiology: Fish Biomechanics*, vol. 23. San Diego, CA: Academic Press.
- Sims, D. W., Wearmouth, V. J., Southall, E. J., Hill, J. M., Moore, P., Rawlinson, K., et al. (2006). Hunt warm, rest cool: bioenergetic strategy underlying diel vertical migration of a benthic shark. *J. Anim. Ecol.* **75**, 176–190.

- Somero, G. N. (2010). The physiology of climate change: how potentials for acclimatization and genetic adaptation will determine 'winners' and 'losers.' *J. Exp. Biol.* **213**, 912–920.
- Standen, E. M. and Lauder, G. V. (2007). Hydrodynamic function of dorsal and anal fins in brook trout (*Salvelinus fontinalis*). *J. Exp. Biol.* **210**, 325–339.
- Stebbing, A. R. D., Turk, S. M. T., Wheeler, A. and Clarke, K. R. (2002). Immigration of southern fish species to south-west England linked to warming of the North Atlantic (1960–2001). *J. Mar. Biol. Assoc. UK.* **82**, 177–180.
- Svendsen, J. C., Steffensen, J. F., Aarestrup, K., Frisk, M., Etzerodt, A. and Jyde, M. (2011). Excess posthypoxic oxygen consumption in rainbow trout (*Oncorhynchus mykiss*): recovery in normoxia and hypoxia. *Can. J. Zool.* **90**, 1–11.
- Syme, D. A. (2006). Functional properties of skeletal muscle. In *Fish Physiology: Fish Biomechanics*, vol. 23 (eds. R. E. Shadwick and G. V. Lauder), pp. 179–240. San Diego, CA: Academic Press.
- Thomson, K. S. (1976). On the heterocercal tail in sharks. *Paleobiology* **2**, 19–38.
- Thomson, K. S. and Simanek, D. E. (1977). Body form and locomotion in sharks. *Am. Zool.* **17**, 343–354.
- Trudel, M., Tremblay, A., Schetagne, R. and Rasmussen, J. B. (2001). Why are dwarf fish so small? An energetic analysis of polymorphism in lake whitefish (*Coregonus clupeaformis*). *Can. J. Fish. Aquat. Sci.* **58**, 394–405.
- van Ginneken, V., Antonissen, E., Muller, U. K., Booms, R., Eding, E., Verreth, J., et al. (2005). Eel migration to the Sargasso: remarkably high swimming efficiency and low energy costs. *J. Exp. Biol.* **208**, 1329–1335.
- Wallman, H. L. and Bennett, W. A. (2006). Effects of parturition and feeding on thermal preference of atlantic stingray, *Dasyatis sabina* (Lesueur). *Environ. Biol. Fish.* **75**, 259–267.
- Walther, G.-R., Post, E., Convey, P., Menzel, A., Parmesan, C., Beebee, T. J. C., et al. (2002). Ecological responses to recent climate change. *Nature* **416**, 389–395.
- Webb, P. W. and Keyes, R. S. (1982). Swimming kinematics of sharks. *Fish. Bull.* **80**, 803–812.
- Wen, L., Weaver, J. C. and Lauder, G. V. (2014). Biomimetic shark skin: design, fabrication, and hydrodynamic function. *J. Exp. Biol.* **217**, 1656–1666.
- Weng, K. and Block, B. (2004). Diel vertical migration of the bigeye thresher shark (*Alopias superciliosus*), a species possessing orbital retia mirabilia. *Fish. Bull.* **102**, 221–229.
- Weng, K., Boustany, A., Pyle, P., Anderson, S., Brown, A. and Block, B. (2007). Migration and habitat of white sharks (*Carcharodon carcharias*) in the eastern Pacific Ocean. *Mar. Biol.* **152**, 877–894.
- Wilga, C. D. and Lauder, G. V. (2000). Three-dimensional kinematics and wake structure of the pectoral fins during locomotion in leopard sharks *Triakis semifasciata*. *J. Exp. Biol.* **203**, 2261–2278.
- Wilga, C. D. and Lauder, G. V. (2001). Functional morphology of the pectoral fins in bamboo sharks, *Chiloscyllium plagiosum*: benthic versus pelagic station holding. *J. Morphol.* **249**, 195–209.
- Wilga, C. D. and Lauder, G. V. (2002). Function of the heterocercal tail in sharks: quantitative wake dynamics during steady horizontal swimming and vertical maneuvering. *J. Exp. Biol.* **205**, 2365–2374.
- Wilga, C. D. and Lauder, G. V. (2004a). Biomechanics of locomotion in sharks, rays and chimeras. In *Biology of Sharks and Their Relatives* (eds. J. C. Carrier, J. A. Musick and M. R. Heithaus), pp. 139–164. Boca Raton, FL: CRC Press.
- Wilga, C. D. and Lauder, G. V. (2004b). Hydrodynamic function of the shark's tail. *Nature* **430**, 850.
- Wurtsbaugh, W. and Li, H. (1985). Diel migrations of *Menidia beryllina* in relation to the distribution of its prey in a large eutrophic lake. *Limnol. Oceanogr.* **30**, 565476.